

NASA TECHNICAL NOTE



NASA TN D-2976

NASA TN D-2976

EDAN COPY: F  
AFWL (W  
KIRTLAND AFI



ONE-DIMENSIONAL NUMERICAL ANALYSIS  
OF THE TRANSIENT RESPONSE  
OF THERMAL PROTECTION SYSTEMS

*by Robert T. Swann, Claud M. Pittman, and James C. Smith*

*Langley Research Center*

*Langley Station, Hampton, Va.*





ONE-DIMENSIONAL NUMERICAL ANALYSIS OF THE TRANSIENT  
RESPONSE OF THERMAL PROTECTION SYSTEMS

By Robert T. Swann, Claud M. Pittman,  
and James C. Smith

Langley Research Center  
Langley Station, Hampton, Va.

NATIONAL AERONAUTICS AND SPACE ADMINISTRATION

---

For sale by the Clearinghouse for Federal Scientific and Technical Information  
Springfield, Virginia 22151 - Price \$2.00

# ONE-DIMENSIONAL NUMERICAL ANALYSIS OF THE TRANSIENT

## RESPONSE OF THERMAL PROTECTION SYSTEMS

By Robert T. Swann, Claud M. Pittman,  
and James C. Smith  
Langley Research Center

### SUMMARY

Differential equations governing the transient response of thermal protection systems to a hyperthermal environment are presented. These equations are expanded into finite-difference equations which are suitable for numerical solution. The equations provide for three layers of different materials, the first two of which may have moving boundaries. Concentrated heat sinks, such as metallic structures, may be located at the back surfaces of the second or third layers or of both layers.

The analysis was developed primarily for charring ablators but is also applicable to impregnated ceramic, subliming, and heat-sink thermal protection systems. The principal difficulty encountered in numerical analysis of charring ablators is the extensive computer time required to obtain solutions. Provision is made in the numerical equations to introduce options which reduce computer time. The errors resulting from these options under various conditions are discussed. Good agreement is obtained between numerical results and exact solutions.

### INTRODUCTION

An adequate thermal protection system may constitute 20 to 30 percent of the total reentry weight for vehicles which must enter the earth's atmosphere at supercircular velocity. Preliminary studies (ref. 1) indicate that charring ablators provide the most efficient thermal protection shield for most of the vehicle. Other materials may be required for certain vehicle areas.

Extensive experimental investigations have been conducted on the performance of charring ablators. (See refs. 2 to 6.) Most of this work is concerned with the overall performance of the material in a given environment. The theoretical analysis of charring ablator systems is very complex by comparison with the analysis of other heat-shield systems, and many approximations and assumptions must be made to obtain solutions. Several procedures for the numerical analysis of the performance of these materials during reentry have been reported. These analyses differ primarily in the treatment of thermal decomposition

processes. In the more rigorous approach (refs. 7 and 8), details of the chemical kinetics of the reactions through the depth of the material are considered. In the more simplified approach to the problem (ref. 9), it is assumed that the decomposition processes occur in a single plane at a temperature which may be fixed or a function of the rate of decomposition. Since it has been shown that the thickness of the decomposition zone is very small compared with the total thickness of the material (ref. 10), this simplifying assumption appears to be valid. In the present analysis, the simplified approach is followed.

The most difficult problem encountered in analysis of the performance of charring ablators is the formulation of a quantitative expression for the rate of char removal. It appears that the char may be removed chemically (oxidation), thermally (sublimation), mechanically (spalling, aerodynamic shear), or by a combination of these methods, depending on the specific material involved. Results of an investigation of oxidation as a mechanism in the performance of charring ablators are presented in reference 11. A theoretical model which predicts spalling of the char, which is observed in some tests, is presented in reference 12. It is also anticipated that aerodynamic shear forces have a pronounced effect on the removal of low-density chars. An analytical program must have considerable flexibility if it is to be suitable for investigation of the various mechanisms of char removal that may be operative.

In this paper, equations are derived for calculating the thermal response of charring ablators to reentry heating conditions. Sufficient options are provided so that not only may all methods of char removal be considered but also, by proper manipulation, the response of impregnated ceramics, subliming ablators, and heat-sink materials to severe heating conditions can be determined. The equations have been programmed for solution by an electronic data processing system, and numerical examples are presented to demonstrate the accuracy of various approximations. The equations presented here are similar to those in reference 9. The primary difference is that in this paper the finite-difference equations are derived for fixed points in a moving coordinate system whereas in reference 9 moving points in a fixed coordinate system are used. The present paper also provides greater flexibility in the boundary conditions which can be imposed.

## SYMBOLS

The units used for the physical quantities defined in this paper are given both in the U.S. Customary Units and in the International System of Units (SI). Factors relating the two systems are given in reference 13.

- A            constant in mass loss rate equation corresponding to specific reaction rate
- B            constant in exponential of mass loss rate equation corresponding to activation energy

b	thickness of layer at which transfer is made between complete equations and boundary equations only (see appendix C)
$C_e$	oxygen concentration by weight external to boundary layer
$C_{i+j}, C_{i+j+m}$	heat capacity of heat sink $(\rho c_p x)_{\text{heat sink}}$
$C_w$	oxygen concentration by weight at wall
$C_1, C_2$	constants of integration (eq. (54))
$c_p$	specific heat
$\bar{c}_p$	specific heat of gaseous products of pyrolysis
D	parameter defined by equation (53), $\frac{x}{k}(\dot{m}_c C_p + m_p \bar{c}_p)$
F	heat-generation function
G	constant in equation (9d)
g	initial temperature distribution
$H_c$	heat of sublimation of char
$h_e$	local enthalpy external to boundary layer
$h_w$	local enthalpy of fluid at wall
$\Delta h_c$	heat of combustion
$\Delta h_f$	heat capacity of coolant
$\Delta h_p$	heat of pyrolysis
i	number of stations in char, including one at each surface
j	number of stations in uncharred material, including one at backface
K	reaction-rate constant for oxidation of char
k	thermal conductivity
$k_{n,n+1}$	thermal conductivity evaluated at temperature of point midway between stations n and n + 1
l	distance between stations

$m$  number of stations in insulation, including one at back surface  
 $\dot{m}$  mass loss rate,  $\alpha_c \dot{m}_c + \alpha_p \dot{m}_p$   
 $\dot{m}_c$  rate of char loss  
 $\dot{m}_p$  rate of loss of uncharred material  
 $\dot{m}_{ox}$  rate at which oxygen diffuses to surface  
 $N_{Le}$  Lewis number  
 $p_w$  total pressure at wall  
 $q$  heating rate  
 $q_{aero}$  net aerodynamic heating rate at the surface (eq. (25b))  
 $q_C$  convective heating rate to a cold wall with no mass transfer  
 $q_{C,net}$  hot-wall convective heating rate corrected for transpiration  
 $q_R$  radiant heating rate  
 $R$  effective nose radius  
 $S(\theta - \bar{T})$  unit step function:  $S = 0, \theta < \bar{T}; S = 1, \theta \geq \bar{T}$   
 $T$  temperature  
 $T_B$  temperature to which back surface radiates  
 $T_n$  temperature at finite-difference stations  
 $\bar{T}_i$  temperature of pyrolysis  
 $\bar{T}_{i+j}, \bar{T}_{i+j+m}$  temperature at which cooling system is activated  
 $\bar{T}_1$  temperature at which char sublimates  
 $t$  time  
 $V$  velocity

$\Delta W_f$	rate of coolant consumption
$x$	thickness
$\bar{x}$	distance from initial outer surface to outer surface of char layer
$y$	distance from initial outer surface of char layer
$Z$	distance from back surface of shield
$\alpha$	absorptivity of char surface
$\alpha_c$	weighting factor for transpiration effectiveness of char mass loss
$\alpha_p$	weighting factor for transpiration effectiveness of pyrolysis products
$\beta$	either 0 or 1 depending on whether transpiration or ablation theory is used
$\epsilon$	emissivity
$\zeta$	transformed coordinate for uncharred material (eq. (23b))
$\eta$	transpiration coefficient
$\theta$	temperature in differential equations
$\lambda$	weight of char removed per unit weight of oxygen
$\xi$	transformed coordinate for char layer (eq. (23a))
$\rho$	density
$\sigma$	Stefan-Boltzmann constant

Subscripts:

$o$	initial value
$i, j, m$	number of stations in first, second, and third layers (see fig. 2)
$n$	integer
$s$	stagnation point
$\infty$	free stream
CALC	calculated by numerical method
EXACT	exact solution

Unprimed symbols refer to char layer unless otherwise specified; single primes refer to uncharred material; double primes refer to insulation.

## ANALYSIS

The thermal protection system that is to be analyzed is shown schematically in figure 1. Although this discussion is confined to a charring ablator system, all the concepts and equations apply equally as well to any other thermal protection system composed of not more than three primary layers. For a charring ablator system, the outer (heated) layer is the char, the center layer contains the uncharred material, and the third layer consists of insulation. Heat sinks can be located at the back of the second or third layers or at both locations.

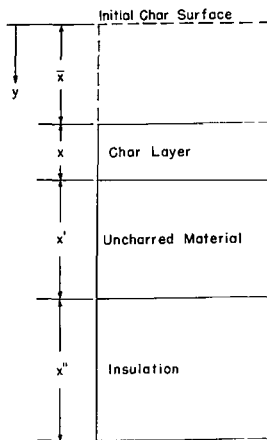


Figure 1.- Schematic diagram of system employing charring ablator.

The outer (char) surface is subjected to aerodynamic heating. The char layer provides both insulation and a high-temperature outer surface for reradiation. The heat passing through this layer is partially absorbed by pyrolysis at the interface between the char layer and the uncharred material, and the remaining heat is conducted into the uncharred material. The gases generated by pyrolysis transpire through the char layer and are injected into the boundary layer. The gases are heated as they pass through the char, and this heat removal from the char layer reduces the quantity of heat conducted to the pyrolysis interface. When these gases are injected into the boundary layer, the convective heat transfer is reduced. This reduction in convective heating is the same effect as that obtained with

simple subliming ablators. In addition to the gases produced by pyrolysis, the carbonaceous residue remaining at the interface adds to the thickness of the char layer. While the processes of pyrolysis, transpiration, and injection are underway, char removal may also be taking place as a result of thermal, chemical, or mechanical processes. Thus the total char thickness may increase or decrease depending on the relative rates of formation and removal of the char. The various processes discussed are related quantitatively in the following sections.

## Differential Equations

It is assumed that thermal properties in a given layer of material are functions only of temperature, that all heat flow is normal to the surface, and that gases transpiring through the char are at the same temperature as the char. Then the governing differential equations (from ref. 9) for the char layer ( $\bar{x} \leq y \leq \bar{x} + x$ ) are as follows:

$$\frac{\partial}{\partial y} \left( k \frac{\partial \theta}{\partial y} \right) + \dot{m}_p \bar{c}_p \frac{\partial \theta}{\partial y} + F = \rho c_p \frac{\partial \theta}{\partial t} \quad (1)$$

Heat conducted      Heat absorbed by      Heat generated      Heat stored  
transpiring gases

for the uncharred layer  $(\bar{x} + x \leq y \leq x_o + x_o')$ ,

$$\frac{\partial}{\partial y} \left( k' \frac{\partial \theta'}{\partial y} \right) = \rho' c_p' \frac{\partial \theta'}{\partial t} \quad (2)$$

and for a layer of insulation  $(x_o + x_o' \leq y \leq x_o + x_o' + x_o'')$ ,

$$\frac{\partial}{\partial y} \left( k'' \frac{\partial \theta''}{\partial y} \right) = \rho'' c_p'' \frac{\partial \theta''}{\partial t} \quad (3)$$

The thicknesses of the layers to which the first two of these equations apply vary with time in a manner which is determined by the boundary conditions.

#### Initial Conditions

The initial temperature distribution is assumed to be given as a function of position:

$$\theta(y, 0) = g(y) \quad (4)$$

The initial mass-transfer rates must also be specified. It should be noted that these values can be other than zero for some cases.

#### Surface Boundary Conditions

Two conditions must be specified at the heated surface. One must determine either the rate of removal of material at the surface or the temperature of the surface; the other is provided by the energy balance.

Surface ablation.- In general, the relative importance of the mechanisms involved in char removal from specific materials is not well established at this time. It has been established, however, that oxidation of the char surface is one important mechanism. Spalling of the char as a result of internal pressure is observed in some cases. Ablation at a given temperature (that is, sublimation) occurs if the heating rate is sufficiently high. Ablation of the surface may also occur as a result of aerodynamic shear stresses.

To provide maximum flexibility, provision is made for the following mechanisms of surface erosion:

- (1) Ablation at a given temperature which may be a function of ablation rate (sublimation)

- (2) Removal of char at a rate which is a given function of time (spalling, aerodynamic shear)
- (3) Removal of char at such a rate that the char thickness is a given function of time (spalling, aerodynamic shear)
- (4) Ablation as a result of a chemical process (oxidation)

For ablation at a given temperature, two cases are considered. In one case, ablation occurs at a fixed temperature. In the other case, the char mass loss rate is an exponential function of the surface temperature. For ablation at a fixed temperature, no surface erosion occurs if the calculated surface temperature is less than the specified ablation temperature. If the calculated surface temperature is higher than the ablation temperature, ablation occurs at a rate sufficient to reduce the temperature to the ablation temperature; that is,  $\dot{m}_c$  is equal to zero for  $T_1 < \bar{T}_1$ , and  $\dot{m}_c$  is calculated from an energy balance at the surface for  $T_1 = \bar{T}_1$ . In the second case, char mass loss rate and surface temperature are related as follows:

$$\dot{m}_c = Ae^{-B/T_1} \quad (5)$$

An equation of this form has some physical significance, because decomposition reactions proceed more rapidly at higher temperatures. By an appropriate selection of A and B, equation (5) yields results similar to those obtained by specifying an ablation temperature.

If the rate of char removal is given function of time

$$\dot{m}_c = f(t) \quad (6)$$

then the rate of char removal is obtained from the input data and the surface temperature is calculated from an energy balance. Such a relation might be used to compare calculated and experimental results when a more basic quantitative relation for the experimental rate of char removal is not available.

If the char thickness is a given function of time

$$x = f(t) \quad (7)$$

then the rate of char removal is calculated from this relation together with the rate of char formation which is calculated from the conditions at the pyrolysis interface. This condition can be used when it is desirable to perform calculations for applications in which the char thickness is known as a function of time even though mechanisms of char removal may be present which cannot be expressed quantitatively.

It has been shown experimentally that oxidation is an important mechanism of char removal. (See ref. 11.) For a half-order reaction, the rate of oxidation of carbon can be determined from the following equation (ref. 14):

$$\dot{m}_c = A e^{-B/T_1} \sqrt{C_w p_w} \quad (8)$$

The pressure at the wall must be specified for subsonic and supersonic flow. However, in hypersonic flow, the pressure can be related to the stagnation heating rate and enthalpy. The stagnation pressure in hypersonic flow is approximately (see ref. 15):

$$p_{w,s} = \frac{11}{12} \rho_\infty V_\infty^2 \quad (9a)$$

Further (from ref. 16),

$$q \propto \sqrt{\frac{\rho_\infty}{R}} V_\infty^3 \quad (9b)$$

and

$$h_e \propto V_\infty^2 \quad (9c)$$

Then,  $p_{w,s}$  can be expressed by the relation

$$p_{w,s} = GR \left( \frac{q_s}{h_{e_s}} \right)^2 \quad (9d)$$

where the constant of proportionality is

$$G = 410.72 \frac{\text{ft}^3\text{-sec}^2\text{-atm}}{\text{lb}^2} = 56.2 \frac{\text{m}^3\text{-sec}^2\text{-atm}}{\text{kg}^2}$$

The pressure at the wall is therefore given by

$$p_w = G \frac{p_w}{p_{w,s}} R \left( \frac{q_s}{h_{e_s}} \right)^2 \quad (9e)$$

where  $\frac{p_w}{p_{w,s}}$  depends on vehicle attitude and body location. The rate at which char is removed by oxygen must be proportional to the net rate at which oxygen diffuses to the surface. From reference 17 this rate is

$$\dot{m}_{\text{ox}} = \frac{N_{\text{Le}}^{0.6} q_{c,\text{net}}}{h_e - h_w} (c_e - c_w) = \frac{\dot{m}_c}{\lambda} \quad (10a)$$

As shown in a subsequent section,  $q_{c,\text{net}}$  is the hot-wall convective heating rate corrected for transpiration (see eq. (13)); that is,

$$q_{C,net} = q_C \left(1 - \frac{h_w}{h_e}\right) \left\{ 1 - (1 - \beta) \left[ 0.724 \frac{h_e}{q_C} (\alpha_c \dot{m}_c + \alpha_p \dot{m}_p) - 0.13 \left(\frac{h_e}{q_C}\right)^2 (\alpha_c \dot{m}_c + \alpha_p \dot{m}_p)^2 \right] - \beta \eta (\alpha_c \dot{m}_c + \alpha_p \dot{m}_p) \frac{h_e}{q_C} \right\} \quad (10b)$$

By eliminating the concentration of oxygen at the wall  $C_w$  in equations (8) and (10a), the rate of removal of char by oxidation is found to be

$$\dot{m}_c = \frac{1}{2} \left\{ - \frac{(h_e - h_w) K^2 p_w}{q_{C,net} \lambda_{Le}^{0.6}} + \sqrt{\left[ \frac{(h_e - h_w) K^2 p_w}{q_{C,net} \lambda_{Le}^{0.6}} \right]^2 + 4 K^2 p_w C_e} \right\} \quad (10c)$$

where  $K = Ae^{-B/T_1}$ .

The equation for a first-order oxidation reaction is obtained similarly. The resulting equation is

$$\dot{m}_c = \frac{K p_w C_e}{1 + \frac{K p_w (h_e - h_w)}{q_{C,net} \lambda_{Le}^{0.6}}} \quad (10d)$$

Surface location.- When char removal occurs, the char surface moves with respect to a coordinate system fixed in the material. The distance between the surface of the char and the initial surface location is given by

$$\bar{x} = \int_0^t \frac{\dot{m}_c}{\rho} dt \quad (11)$$

The thickness of the char at any time is equal to the initial char thickness, plus the thickness of char formed by pyrolysis, less the thickness of char removed; that is,

$$x = x_0 + \int_0^t \frac{\dot{m}_p}{\rho' - \rho} dt - \int_0^t \frac{\dot{m}_c}{\rho} dt \quad (12)$$

Surface energy balance.- The heat input consists of convective and radiant heating. This energy must be accommodated at the surface by a combination of four mechanisms:

- (1) Blocking by mass transfer into the boundary layer
- (2) Reradiation or reflection from the surface
- (3) Conduction into the material
- (4) Sublimation of the char

The effect of mass transfer on heat transfer has been studied extensively. With low-mass-transfer rates it is found that the reduction in heat-transfer rate is directly proportional to the product of the mass-transfer rate and the enthalpy difference across the boundary layer. With high-mass-transfer rates, which may occur when a large fraction of the heat input is radiant, the linear approximation is no longer adequate and it is necessary to use a higher order approximation. A second-degree approximation is derived in appendix A.

The surface energy balance, expressed in a form in which either approximation to the blocking effectiveness can be selected, is as follows:

$$\underbrace{q_C}_{\text{Cold wall convective heating rate}} + \underbrace{\left(1 - \frac{h_w}{h_e}\right)}_{\text{Hot wall correction}} \underbrace{\left\{ 1 - (1 - \beta) \left[ 0.724 \frac{h_e}{q_C} (\alpha_c \dot{m}_c + \alpha_p \dot{m}_p) - 0.13 \left( \frac{h_e}{q_C} \right)^2 (\alpha_c \dot{m}_c + \alpha_p \dot{m}_p)^2 \right] - \beta \eta (\alpha_c \dot{m}_c + \alpha_p \dot{m}_p) \frac{h_e}{q_C} \right\}}_{\text{Aerodynamic blocking}}$$

Net convective heating rate

$$+ \underbrace{\alpha q_R}_{\text{Radiative heating rate}} + \underbrace{\left[ 1 - s(\theta - \bar{T}_1) \right] \dot{m}_c \Delta h_c}_{\text{Combustive heating rate}} = \underbrace{\sigma \epsilon_1 \theta_1^4}_{\text{Reradiation}} - \underbrace{k \frac{\partial \theta}{\partial y}}_{\text{Conduction to interior}} + \underbrace{s(\theta - \bar{T}_1) \dot{m}_c H_c}_{\text{Heat of sublimation of char}} \tag{13}$$

If transpiration theory (second-degree approximation, appendix A) is used,  $\beta$  is equal to zero. For linear ablation theory,  $\beta$  is equal to 1. In either case, the heat absorbed by vaporization of the char  $H_c$  and the heat of combustion of the char  $\Delta h_c$  are considered separately. The coefficients  $\alpha_c$  and  $\alpha_p$  can be used to differentiate between the blocking effectiveness of the gases produced at the surface and at the pyrolysis interface. Evaluation of these coefficients is discussed briefly in appendix A.

The heat transfer to the outer surface is assumed to be a given function of time and consists of the cold-wall convective heating rate  $q_C$  and the radiant heating rate  $q_R$  incident on the surface. These two components must be specified separately because mass transfer at the surface blocks part of the aerodynamic heating but, in general, has no effect on radiant heating. Additional terms can easily be included in equation (13) to account for other

phenomena which may affect the heat balance at the char surface. For example, reference 18 discusses a gas-phase combustion in the boundary layer involving the gases of pyrolysis. This effect has not been clearly identified at the Langley Research Center and is, therefore, not included in the equation. However, phenomena such as this may be important in some cases and their existence should certainly be considered.

Equation (13) is normally used in this analysis as the boundary condition on the temperature at the outer surface. However, when  $\theta$  is equal to the sublimation temperature  $\bar{T}_1$ , the specified sublimation temperature provides the boundary condition on the temperature and equation (13) is used to calculate the rate of ablation  $\dot{m}_c$ .

#### Pyrolysis-Interface Boundary Condition

Energy balance.- The heat conducted to the pyrolysis interface must be either absorbed by pyrolysis reactions or conducted into the uncharred material; that is, at  $y = \bar{x} + x$ ,

$$-k \frac{\partial \theta}{\partial y} = \dot{m}_p \Delta h_p - k' \frac{\partial \theta'}{\partial y} \quad (14)$$

In addition, the temperatures in the char and in the uncharred material must be equal at the interface; that is, at  $y = \bar{x} + x$ ,

$$\theta = \theta' \quad (15)$$

Pyrolysis rate.- Two approaches are available for calculating the rate of pyrolysis. In the first approach, it is assumed that pyrolysis occurs at a given temperature  $\bar{T}_1$ . If

$$\theta_{\bar{x}+x} < \bar{T}_1 \quad (16a)$$

then

$$\dot{m}_p = 0 \quad (16b)$$

If

$$\theta_{\bar{x}+x} = \bar{T}_1$$

the temperature is known and equation (14) is used to calculate the rate of pyrolysis.

In an alternate approach, it is assumed that the rate of pyrolysis is a known function of temperature, for example

$$\dot{m}_p = A'e^{-B'/\theta_{\bar{x}+x}} \quad (17)$$

when

$$\theta_{\bar{x}+x} < \bar{T}_i$$

In this case, equations (14) and (17) are solved for both temperature and pyrolysis rate. The value of  $\bar{T}_i$  is still specified, and if this temperature is reached, the pyrolysis rate is determined only from equation (14) so that this temperature is not exceeded.

Pyrolysis-interface location.- As pyrolysis occurs, the interface between the char layer and the uncharred material moves with respect to a fixed coordinate. Its distance from the initial char surface location is

$$\bar{x} + x = x_0 + \int_0^t \frac{\dot{m}_p}{\rho' - \rho} dt \quad (18)$$

The instantaneous thickness of the uncharred material is

$$x' = x'_0 - \int_0^t \frac{\dot{m}_p}{\rho' - \rho} dt \quad (19)$$

#### Boundary Conditions at Back Surface of Ablation Material

A number of conditions can be imposed at the back surface of the ablation material, depending on whether additional insulation is provided or some provision is made for temperature control. Whether insulation is used or not, the ablation material may be attached to a thermally thin plate which functions as a concentrated heat sink.

Three-layer system.- If insulation is used, the temperature of the ablation material is equal to the temperature of the insulation at their interface.

$$\theta'_{x_0+x'_0} = \theta''_{x_0+x'_0} \quad (20a)$$

From an energy balance at the back surface of the ablation material,

$$-k' \frac{\partial \theta'}{\partial y} = C_{i+j} \frac{\partial \theta'}{\partial t} - k'' \frac{\partial \theta''}{\partial y} \quad (20b)$$

Two-layer system.- If no insulating layer is used, the back surface can be assumed to be perfectly insulated, cooled at a given temperature, or may exchange radiation with a sink of known temperature in the interior of the structure. An energy balance yields the following equation:

$$-k' \frac{\partial \theta'}{\partial y} = C_{i+j} \frac{\partial \theta'}{\partial y} + S (\theta' - \bar{T}_{i+j}) \Delta W_f \Delta h_f + \sigma \epsilon_{i+j} \left[ (\theta')^4 - T_B^4 \right] \quad (21)$$

The temperature at which the cooling system is activated is  $\bar{T}_{i+j}$ . The choice of conditions is accomplished by making the inapplicable terms equal to zero (that is,  $C_{i+j} = 0$  and/or  $\bar{T}_{i+j} > \theta'$  and/or  $\epsilon_{i+j} = 0$ ).

#### Boundary Condition at Back Surface of Insulating Material

If an insulating material is used behind the ablating material, the boundary condition at the back surface ( $y = x_0 + x_0' + x_0''$ ) is similar to equation (21); that is,

$$-k'' \frac{\partial \theta''}{\partial y} = C_{i+j+m} \frac{\partial \theta''}{\partial t} + S (\theta'' - \bar{T}_{i+j+m}) \Delta W_f \Delta h_f + \sigma \epsilon_{i+j+m} \left[ (\theta'')^4 - T_B^4 \right] \quad (22)$$

#### Transformation of Coordinates

The equations derived in the preceding discussion are similar to those presented in reference 9. In reference 9, these equations are expressed in finite-difference form and solved in a fixed coordinate system. To maintain a fixed number of stations in layers of varying thicknesses, it is necessary to change the locations of the stations and to interpolate to determine the temperatures at the new locations after each step in the calculation. This procedure not only increases the time required to perform the computations, but also introduces a small error in each step of the calculation. This difficulty can be eliminated by transforming the equations to a coordinate system in which the finite-difference stations remain fixed, and the coordinates themselves move to accommodate the changes in the locations of the surfaces of the different materials.

The  $y$ -coordinate can be transformed to  $\xi$ - and  $\zeta$ -coordinates in the char and uncharred layers, respectively, by using the following equations:

$$\xi = \frac{y - \int_0^t \frac{\dot{m}_c}{\rho} dt}{x} \quad (23a)$$

$$\zeta = \frac{y - x_0 - \int_0^t \frac{\dot{m}_p}{\rho' - \rho} dt}{x'} \quad (23b)$$

In this coordinate system the outer surface remains fixed at  $\xi = 0$ . The interface is located at  $\xi = 1$  in the char and at  $\zeta = 0$  in the uncharred material. The back surface of the uncharred material is located at  $\zeta = 1$ . A number of advantages result from the use of this double transformation. First, the char always extends from  $\xi = 0$  to  $\xi = 1$ . Therefore, the temperatures tend to be more nearly steady state than would be the case with a coordinate system fixed at the surface only. A second advantage is the positive location of the pyrolysis interface. A similar transformation would also be very beneficial in locating the center of the reaction zone when the pyrolysis reactions are considered in detail. Because the reaction zone is typically very thin, a very fine finite-difference network is required to analyze it. With transformations similar to those here, the center of the reaction zone can be located, and the fine network can be restricted to this region rather than covering the entire range of possible reaction-zone locations.

In the transformed coordinate system, equations (1) and (2) are as follows (for the char layer and uncharred layer, respectively):

$$\frac{1}{x^2} \frac{\partial}{\partial \xi} \left( k \frac{\partial \theta}{\partial \xi} \right) + \frac{1}{x} \frac{\partial \theta}{\partial \xi} \left[ \dot{m}_c c_p + \dot{m}_p \bar{c}_p + \xi \left( \frac{\dot{m}_p \rho}{\rho' - \rho} - \dot{m}_c \right) c_p \right] + F = \rho c_p \frac{\partial \theta}{\partial t} \quad (24a)$$

$$\frac{1}{(x')^2} \frac{\partial}{\partial \zeta} \left( k' \frac{\partial \theta'}{\partial \zeta} \right) + \frac{1}{x'} \frac{\dot{m}_p \rho' c_p'}{\rho' - \rho} (1 - \zeta) \frac{\partial \theta'}{\partial \zeta} = \rho' c_p' \frac{\partial \theta'}{\partial t} \quad (24b)$$

The boundary conditions are as follows:

At  $\xi = 0$ ,

$$q_{aero} = \sigma \epsilon_1 \theta^4 - \frac{k}{x} \frac{\partial \theta}{\partial \xi} + \dot{m}_c \left[ S (\theta - \bar{T}_1) (H_c + \Delta h_c) - \Delta h_c \right] \quad (25a)$$

where

$$q_{aero} = \alpha q_R + q_C \left( 1 - \frac{h_w}{h_e} \right) \left\{ 1 - (1 - \beta) \left[ 0.724 \frac{h_e}{q_C} (\alpha_c \dot{m}_c + \alpha_p \dot{m}_p) - 0.13 \left( \frac{h_e}{q_C} \right)^2 (\alpha_c \dot{m}_c + \alpha_p \dot{m}_p)^2 \right] - \beta \eta (\alpha_c \dot{m}_c + \alpha_p \dot{m}_p) \frac{h_e}{q_C} \right\} \quad (25b)$$

at  $\xi = 1$ ,  $\zeta = 0$ ,

$$\theta = \theta' \quad (26a)$$

and

$$-\frac{k}{x} \frac{\partial \theta}{\partial \xi} = \dot{m}_p \Delta h_p - \frac{k'}{x'} \frac{\partial \theta'}{\partial \zeta} \quad (26b)$$

and at  $\zeta = 1$  for only two layers, the condition at the back surface ( $y = x_0 + x'_0$ ) is

$$-\frac{k'}{x'} \frac{\partial \theta'}{\partial \zeta} = C_{i+j} \frac{\partial \theta'}{\partial t} + S(\theta' - \bar{T}_{i+j}) \Delta W_f \Delta h_f + \sigma \epsilon_{i+j} \left[ (\theta')^4 - T_B^4 \right] \quad (27)$$

When three layers are used, the conditions at the back of the second layer are

$$\theta' = \theta'' \quad (28a)$$

and

$$-\frac{k'}{x'} \frac{\partial \theta'}{\partial \zeta} = C_{i+j} \frac{\partial \theta'}{\partial t} - k'' \frac{\partial \theta''}{\partial y} \quad (28b)$$

If three layers are used, the condition at the back surface ( $y = x_0 + x'_0 + x''_0$ ) is

$$-k'' \frac{\partial \theta''}{\partial y} = C_{i+j+m} \frac{\partial \theta''}{\partial t} + S(\theta'' - \bar{T}_{i+j+m}) \Delta W_f \Delta h_f + \sigma \epsilon_{i+j+m} \left[ (\theta'')^4 - T_B^4 \right] \quad (29)$$

### Finite-Difference Equations

The locations of the finite-difference stations are shown in figure 2.

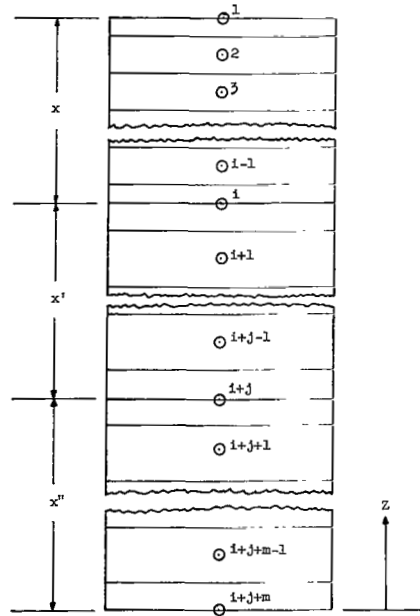


Figure 2.- Location of finite-difference stations.

The methods used to change the differential equations to finite-difference form are given in appendix B. A summary of the finite-difference equations obtained by these methods is presented here.

The equation at the first station (eq. (B25)) is

$$k_{1,2} \frac{T_2 - T_1}{\lambda} + q_{\text{aero}} - \sigma \epsilon_1 T_1^4 - \dot{m}_c \left[ S(T_1 - \bar{T}_1)(H_c + \Delta h_c) - \Delta h_c \right] + \frac{1}{12} (-11T_1 + 18T_2 - 9T_3 + 2T_4) (\dot{m}_c c_p + \dot{m}_p \bar{c}_p) + \frac{\lambda}{2} F = \rho c_p \frac{\lambda}{2} \frac{\Delta T_1}{\Delta t} \quad (30)$$

The equations for the first layer (eqs. (B9) and (B10)) are

$$k_{n-1,n} \frac{T_{n-1} - T_n}{\lambda} - k_{n,n+1} \frac{T_n - T_{n+1}}{\lambda} + \frac{1}{6} (6T_{n+1} - 3T_n - 2T_{n-1} - T_{n+2}) \left[ \dot{m}_c c_p + \dot{m}_p \bar{c}_p + \frac{n-1}{i-1} \left( \frac{\dot{m}_p \rho}{\rho' - \rho} - \dot{m}_c \right) c_p \right] + \lambda F = \lambda \rho c_p \frac{\Delta T_n}{\Delta t} \quad (2 \leq n \leq i-2) \quad (31)$$

and

$$k_{n-1,n} \frac{T_{n-1} - T_n}{\lambda} - k_{n,n+1} \frac{T_n - T_{n+1}}{\lambda} + \frac{1}{6} (2T_{n+1} + 3T_n - 6T_{n-1} + T_{n-2}) \left[ \dot{m}_c c_p + \dot{m}_p \bar{c}_p + \frac{n-1}{i-1} \left( \frac{\dot{m}_p \rho}{\rho' - \rho} - \dot{m}_c \right) c_p \right] + \lambda F = \rho c_p \lambda \frac{\Delta T_n}{\Delta t} \quad (n = i-1) \quad (32)$$

The equation at the pyrolysis interface (eq. (B30)) is

$$2 \left( k'_{i,i+1} \frac{T_{i+1} - T_i}{\lambda'} - k_{i-1,i} \frac{T_i - T_{i-1}}{\lambda} \right) + \lambda F + \dot{m}_p \left\{ \left( \bar{c}_p + \frac{c_p \rho}{\rho' - \rho} \right) \left[ \frac{1}{6} (11T_i - 18T_{i-1} + 9T_{i-2} - 2T_{i-3}) \right] + \frac{c_p \rho'}{\rho' - \rho} \left[ \frac{1}{6} (-11T_i + 18T_{i+1} - 9T_{i+2} + 2T_{i+3}) \right] - 2\Delta h_p \right\} = (\rho c_p \lambda + \rho' c_p \lambda') \frac{\Delta T_i}{\Delta t} \quad (33)$$

The equations for the second layer (eqs. (B15) and (B16)) are

$$\begin{aligned}
& k'_{n-1,n} \frac{T_{n-1} - T_n}{\lambda'} - k'_{n,n+1} \frac{T_n - T_{n+1}}{\lambda'} \\
& + \frac{1}{6} (6T_{n+1} - 3T_n - 2T_{n-1} - T_{n+2}) \frac{i+j-n}{j} \frac{\dot{m}_p \rho' c'_p}{\rho' - \rho} = \lambda' \rho' c'_p \frac{\Delta T_n}{\Delta t}
\end{aligned}
\tag{34}$$

( $i + 1 \leq n \leq i + j - 2$ )

and

$$\begin{aligned}
& k'_{n-1,n} \frac{T_{n-1} - T_n}{\lambda'} - k'_{n,n+1} \frac{T_n - T_{n+1}}{\lambda'} \\
& + \frac{1}{6} (2T_{n+1} + 3T_n - 6T_{n-1} + T_{n-2}) \frac{i+j-n}{j} \frac{\dot{m}_p \rho' c'_p}{\rho' - \rho} = \lambda' \rho' c'_p \frac{\Delta T_n}{\Delta t}
\end{aligned}
\tag{35}$$

( $n = i + j - 1$ )

The equations at the back of the second layer are for two layers (eq. (B33))

$$\begin{aligned}
& k'_{i+j-1,i+j} \frac{T_{i+j-1} - T_{i+j}}{\lambda'} - \sigma \epsilon_{i+j} (T_{i+j}^h - T_B^h) - S (T_{i+j} - \bar{T}_{i+j}) \Delta W_f \Delta h_f \\
& = \left( \rho' c'_p \frac{\lambda'}{2} + C_{i+j} \right) \frac{\Delta T_{i+j}}{\Delta t}
\end{aligned}
\tag{36}$$

and, for three layers (eq. (B36))

$$\begin{aligned}
& k'_{i+j-1,i+j} \frac{T_{i+j-1} - T_{i+j}}{\lambda'} - k''_{i+j,i+j+1} \frac{T_{i+j} - T_{i+j+1}}{\lambda''} \\
& = \left( \rho' c'_p \frac{\lambda'}{2} + \rho'' c''_p \frac{\lambda''}{2} + C_{i+j} \right) \frac{\Delta T_{i+j}}{\Delta t}
\end{aligned}
\tag{37}$$

The equation for the third layer (eq. (B19))

$$k''_{n-1,n} \frac{T_{n-1} - T_n}{\lambda''} - k''_{n,n+1} \frac{T_n - T_{n+1}}{\lambda''} = \rho'' c''_p \lambda'' \frac{\Delta T_n}{\Delta t}
\tag{38}$$

The equation at the back surface of the third layer (eq. (B39)) is

$$\begin{aligned}
& k''_{i+j+m-1, i+j+m} \frac{T_{i+j+m-1} - T_{i+j+m}}{\lambda''} \\
& = \sigma \epsilon_{i+j+m} (T_{i+j+m}^4 - T_B^4) + S(T_{i+j+m} - \bar{T}_{i+j+m}) \Delta W_f \Delta h_f + \left( \rho'' c_p'' \frac{\lambda''}{2} + C_{i+j+m} \right) \frac{\Delta T_{i+j+m}}{\Delta t}
\end{aligned} \tag{39}$$

In some cases it is desirable to use the so-called thin-layer options, presented in appendix C, because of the considerable saving of computer time involved in their use. When these options are used, the layer in question is divided into two half-elements and the interior stations in the layer are no longer considered. The first layer is considered "thin" when  $x$  is less than some prescribed thickness  $b$ , and the second layer is considered "thin" when  $x'$  is less than some prescribed thickness  $b'$ . The finite-difference equations used with the thin-layer options are as follows.

At the front surface, method 1 gives the following equation when  $x \leq b$  (eq. (C1))

$$\begin{aligned}
& k_{1,i} \frac{T_i - T_1}{x} + q_{aero} - \sigma \epsilon_1 T_1^4 - \dot{m}_c \left[ S(T_1 - \bar{T}_1)(H_c + \Delta h_c) - \Delta h_c \right] \\
& + \frac{T_i - T_1}{2} (\dot{m}_c c_p + \dot{m}_p \bar{c}_p) + \frac{x}{2} F = \rho c_p \frac{x}{2} \frac{\Delta T_1}{\Delta t}
\end{aligned} \tag{40}$$

The equations at the interface are, for  $x \leq b$  and  $x' > b'$  (eq. (C2))

$$\begin{aligned}
& 2k'_{i,i+1} \frac{T_{i+1} - T_i}{\lambda'} - 2k_{1,i} \frac{T_i - T_1}{x} + xF + \dot{m}_p \left\{ \left( \bar{c}_p + \frac{\rho c_p}{\rho' - \rho} \right) (T_i - T_1) \right. \\
& \left. + \frac{c'_p \rho'}{\rho' - \rho} \left[ \frac{1}{6} (-11T_i + 18T_{i+1} - 9T_{i+2} + 2T_{i+3}) \right] - 2\Delta h_p \right\} = (\rho c_p x + \rho' c'_p \lambda') \frac{\Delta T_1}{\Delta t}
\end{aligned} \tag{41}$$

for  $x \leq b$  and  $x' \leq b'$  (eq. (C3))

$$\begin{aligned}
& 2k'_{i,i+j} \frac{T_{i+j} - T_i}{x'} - 2k_{1,i} \frac{T_i - T_1}{x} + xF + \dot{m}_p \left[ \left( \bar{c}_p + \frac{\rho c_p}{\rho' - \rho} \right) (T_i - T_1) \right. \\
& \left. + \frac{c'_p \rho'}{\rho' - \rho} (T_{i+j} - T_i) - 2\Delta h_p \right] = (\rho c_p x + \rho' c'_p x') \frac{\Delta T_1}{\Delta t}
\end{aligned} \tag{42}$$

and for  $x > b$  and  $x' \leq b'$  (eq. (C4))

$$\begin{aligned}
& 2k'_{i,i+j} \frac{T_{i+j} - T_i}{x'} - 2k_{i-1,i} \frac{T_i - T_{i-1}}{l} + lF \\
& + \dot{m}_p \left\{ \left( \bar{c}_p + \frac{\rho c_p}{\rho' - \rho} \right) \left[ \frac{1}{6} (11T_i - 18T_{i-1} + 9T_{i-2} - 2T_{i-3}) \right] \right. \\
& \left. + \frac{c'_p \rho'}{\rho' - \rho} (T_{i+j} - T_i) - 2\Delta h_p \right\} = (\rho c_p l + \rho' c'_p x') \frac{\Delta T_i}{\Delta t} \quad (43)
\end{aligned}$$

The equation at the back surface of the second layer for two layers (eq. (C5)) is

$$\begin{aligned}
k'_{i,i+j} \frac{T_i - T_{i+j}}{x'} - \sigma \epsilon_{i+j} (T_{i+j}^h - T_B^h) - S(T_{i+j} - \bar{T}_{i+j}) \Delta W_f \Delta h_f \\
= \left( \rho' c'_p \frac{x'}{2} + C_{i+j} \right) \frac{\Delta T_{i+j}}{\Delta t} \quad (44)
\end{aligned}$$

and for three layers (eq. (C6)) is

$$k'_{i,i+j} \frac{T_i - T_{i+j}}{x'} - k''_{i+j,i+j+1} \frac{T_{i+j} - T_{i+j-1}}{l''} = \left( \rho' c'_p \frac{x'}{2} + \rho'' c''_p \frac{l''}{2} + C_{i+j} \right) \frac{\Delta T_{i+j}}{\Delta t} \quad (45)$$

#### Calculation of Temperatures at Fixed Points

It is possible to calculate the temperature at any number of fixed points  $Z_n$  where  $Z$  is the distance from the back surface. (See fig. 2.) The temperature at  $Z_n$  is calculated as follows (by using linear interpolation):

When

$$0 < Z_n \leq x''$$

find station  $N$  such that

$$(i + j + m - N)l'' \geq Z_n \geq (i + j + m - N - 1)l''$$

Then

$$T(Z_n) = T_N + (T_N - T_{N+1}) \frac{Z_n - (i + j + m - N)l''}{l''} \quad (46)$$

When

$$x'' \leq Z_n \leq x' + x''$$

find  $N$  such that

$$x'' + (i + j - N)l' \geq Z_n \geq x'' + (i + j - N - 1)l'$$

Then

$$T(Z_n) = T_N + (T_N - T_{N+1}) \frac{Z_n - x'' - (i + j - N)l'}{l'} \quad (47)$$

When

$$x' + x'' \leq Z_n \leq x + x' + x''$$

find  $N$  such that

$$x' + x'' + (i - N)l \geq Z_n \geq x' + x'' + (i - N - 1)l$$

Then

$$T(Z_n) = T_N + (T_N - T_{N+1}) \frac{Z_n - x' - x'' - (i - N)l}{l} \quad (48)$$

If the outside surface moves past the largest  $Z_n$  because of ablation of the surface, then the temperature at this point is meaningless and is, therefore, not calculated.

## RESULTS AND DISCUSSION

Comparisons have been made of the numerical results obtained when the various options presented in this report are used. Comparisons with exact solutions have also been made. The results of these studies are presented and discussed in the following sections.

### Comparison With Exact Solutions

The accuracy of the numerical analysis is determined for two cases for which exact solutions are available. One case provides an exact solution for a homogeneous nonablating heat-sink material subjected to a suddenly applied constant heating rate. The other case is for quasi-steady-state ablation. In both cases, constant material property values and environmental values are used and reradiation from the surface is not considered.

Heat-sink case.- The exact solution for the heat-sink case is obtained from equation (A11) of reference 19. When written with the symbols used in this paper, the equation is

$$T\left(\frac{y}{x+x'}, t\right) - T_0 = \frac{q(x+x')}{k} \left\{ \frac{kt}{\rho c_p (x+x')^2} + \frac{1}{2} \left(1 - \frac{y}{x+x'}\right)^2 - \frac{1}{6} - \frac{2}{\pi^2} \sum \frac{(-1)^n}{n^2} \cos \left[ n\pi \left(1 - \frac{y}{x+x'}\right) \right] \exp \left[ n^2 \pi^2 \frac{kt}{\rho c_p (x+x')^2} \right] \right\} \quad (49)$$

The values of  $q$  and material properties used to obtain a solution to equation (49) are given in table I. These values do not represent a real material but were chosen to simplify the calculation.

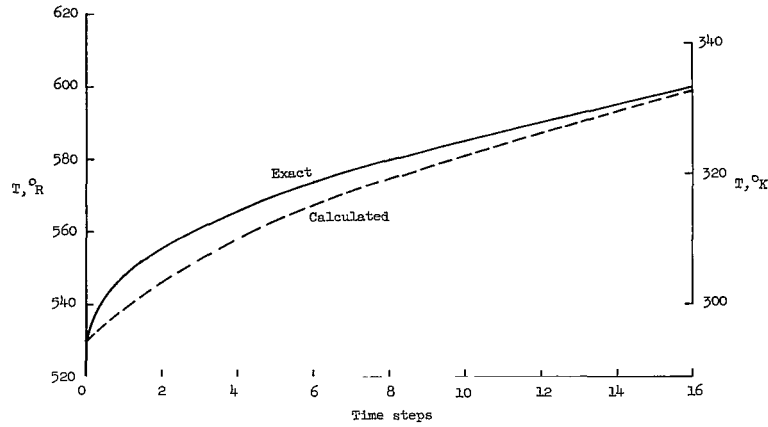
TABLE I.- VALUES USED FOR HEAT-SINK EXACT SOLUTION

Quantity	Value in U.S. customary units	Value in SI units
$q$ . . . . .	100 Btu/ft <sup>2</sup> -sec	1135 kW/m <sup>2</sup>
$t$ . . . . .	0.1 ft	3.048 cm
$k$ . . . . .	0.01 Btu/ft-sec-°R	62.4 W/m-°K
$\rho$ . . . . .	10 lb/ft <sup>3</sup>	160 kg/m <sup>3</sup>
$c_p$ . . . . .	0.1 Btu/lb-°R	0.4184 kJ/kg-°K
$T_0$ . . . . .	530° R	294° K

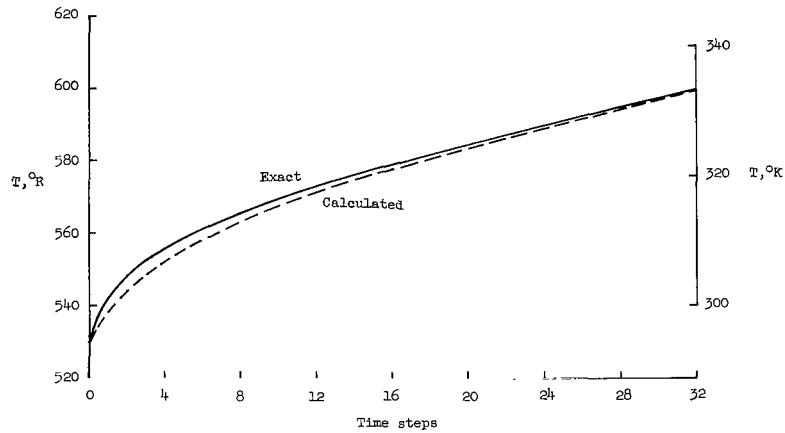
When a comparison is made between surface temperature histories calculated from this equation and calculations made with the finite-difference equations, the following results are obtained. At the heated surface  $\frac{y}{x+x'} = 0$ , the error is about -0.4° R (-0.2° K) out of about 1863° R (1035° K) when  $T_0$  is 530° R (294° K).

Figure 3 shows a comparison between the finite-difference solutions and the exact solution for the first few time steps of the calculations. The calculations shown in figure 3(a) use a time interval of 1/4096 second. It can be seen that after about 16 time steps (1/256 second each), the agreement is adequate.

The results obtained when the time interval is cut in half are shown in figure 3(b). It can be seen that the error in surface temperature is reduced considerably for the same heating period.



(a)  $\Delta t = 1/4096$  second.



(b)  $\Delta t = 1/8192$  second.

Figure 3.- Comparison of surface temperatures for initial time steps.

Quasi-steady-state ablation case.- A quasi-steady-state case is one in which the front surface and pyrolysis interface recede at the same rate; thus, the char thickness is constant. If conditions are also chosen such that there is no heat transfer into the uncharred layer, an exact solution can be obtained.

The transformed heat balance equation for the first layer is (eq. (24a))

$$\frac{1}{x^2} \frac{\partial}{\partial \xi} \left( k \frac{\partial \theta}{\partial \xi} \right) + \frac{1}{x} \frac{\partial \theta}{\partial \xi} \left[ \dot{m}_c c_p + \dot{m}_p \bar{c}_p + \xi \left( \frac{\dot{m}_p \rho}{\rho_p - \rho} - \dot{m}_c \right) c_p \right] + F = \rho c_p \frac{\partial \theta}{\partial t}$$

With quasi-steady-state ablation,  $x$ ,  $\dot{m}_p$ , and  $\dot{m}_c$  are constant. Further,

$$\left. \begin{aligned} \frac{\dot{m}_p \rho}{\rho^* - \rho} - \dot{m}_c &= 0 \\ \frac{\partial \theta}{\partial t} &= 0 \end{aligned} \right\} \quad (50)$$

Therefore equation (24a) becomes (with  $F = 0$ ):

$$\frac{1}{x^2} \frac{d}{d\xi} \left( k \frac{d\theta}{d\xi} \right) + \frac{1}{x} \frac{d\theta}{d\xi} (\dot{m}_c c_p + \dot{m}_p \bar{c}_p) = 0 \quad (51)$$

Then with constant  $k$ ,  $\bar{c}_p$  and  $c_p$ , equation (51) can be written

$$\frac{d^2 \theta}{d\xi^2} + D \frac{d\theta}{d\xi} = 0 \quad (52)$$

where

$$D = \frac{x}{k} (\dot{m}_c c_p + \dot{m}_p \bar{c}_p) \quad (53)$$

The solution of equation (52) is ( $\theta$  being replaced by  $T$ )

$$T = C_1 + C_2 e^{-D\xi} \quad (54)$$

and  $C_1$  and  $C_2$  can be found from the boundary conditions:

$$T = T_c \quad (\xi = 0)$$

$$T = T_p \quad (\xi = 1)$$

The final solution is

$$T = \frac{T_p - T_c e^{-D} + (T_c - T_p) e^{-D\xi}}{1 - e^{-D}} \quad (55)$$

To determine the mass loss rates  $\dot{m}_c$  and  $\dot{m}_p$ , and the char thickness  $x$  associated with this equation, the following equations are used:

$$\left. \begin{aligned} \frac{\dot{m}_p \rho}{\rho' - \rho} &= \dot{m}_c \\ \left. \frac{\partial \theta}{\partial \xi} \right]_{\xi=0} &= \frac{x}{k} \left( \dot{m}_c H_c - q_{aero} \right) \\ \left. \frac{\partial \theta}{\partial \xi} \right]_{\xi=1} &= - \frac{\dot{m}_p \Delta h_p x}{k} \end{aligned} \right\} \quad (56)$$

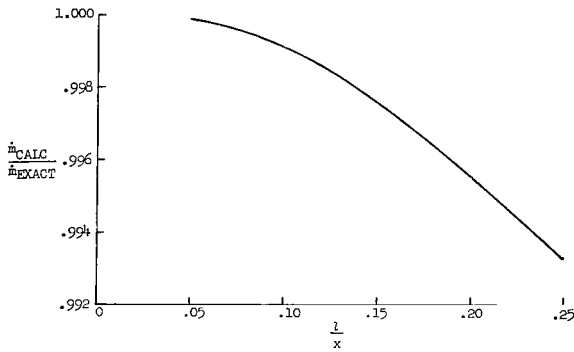
In the last equation, it is assumed that  $\left. \frac{\partial \theta}{\partial \xi} \right]_{\xi=0}$  is negligibly small; that is, there is no heat flow into the second layer. By solving equations (55) and (56) for  $\dot{m}_c$ ,  $\dot{m}_p$ , and  $x$ , the following equations are obtained:

$$\left. \begin{aligned} \dot{m}_c &= \frac{\rho}{\rho' - \rho} \left\{ \frac{q_{aero}}{\left( \bar{c}_p + \frac{\rho c_p}{\rho' - \rho} \right) (T_c - T_p) + \Delta h_p + \frac{\rho H_c}{\rho' - \rho}} \right\} \\ \dot{m}_p &= \frac{q_{aero}}{\left( \bar{c}_p + \frac{\rho c_p}{\rho' - \rho} \right) (T_c - T_p) + \Delta h_p + \frac{\rho H_c}{\rho' - \rho}} \\ x &= \frac{k}{q_{aero}} \left( T_c - T_p + \frac{\Delta h_p + \frac{\rho H_c}{\rho' - \rho}}{\bar{c}_p + \frac{\rho c_p}{\rho' - \rho}} \right) \log_e \left[ \frac{\left( \bar{c}_p + \frac{\rho c_p}{\rho' - \rho} \right) (T_c - T_p)}{\Delta h_p} + 1 \right] \end{aligned} \right\} \quad (57)$$

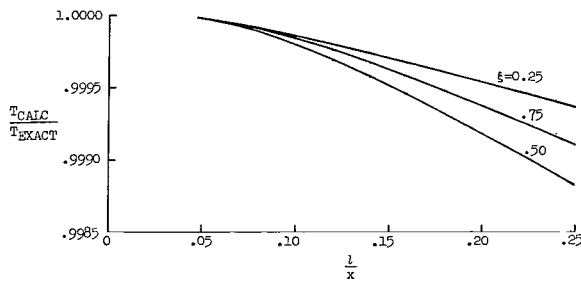
The values of  $q_{aero}$  and material properties used to obtain a solution to equation (55) (by using eqs. (53) and (57)) are given in table II. These values do not represent a real material but were chosen to simplify the calculation.

TABLE II.-- VALUES USED FOR QUASI-STEADY-STATE EXACT SOLUTION

Quantity	Value in U.S. Customary Units	Value in SI Units
q . . . . .	69.3 Btu/ft <sup>2</sup> -sec	785 kW/m <sup>2</sup>
k . . . . .	1.0 × 10 <sup>-4</sup> Btu/ft-sec-°R	0.624 W/m-°K
ρ . . . . .	20 lb/ft <sup>3</sup>	320 kg/m <sup>3</sup>
ρ' . . . . .	40 lb/ft <sup>3</sup>	640 kg/m <sup>3</sup>
c <sub>p</sub> . . . . .	0.5 Btu/lb-°R	2.09 kJ/kg-°K
$\bar{c}_p$ . . . . .	0.5 Btu/lb-°R	2.09 kJ/kg-°K
T <sub>1</sub> . . . . .	4000° R	2222 °K
T <sub>i</sub> . . . . .	1000° R	556 °K
Δh <sub>p</sub> . . . . .	1000 Btu/lb	2.324 MJ/kg
H <sub>c</sub> . . . . .	1000 Btu/lb	2.324 MJ/kg



(a) Mass loss rate.



(b) Temperature.

Figure 4.- Error in quasi-steady-state solution ( $x = 0.01$  ft =  $0.3048$  cm).

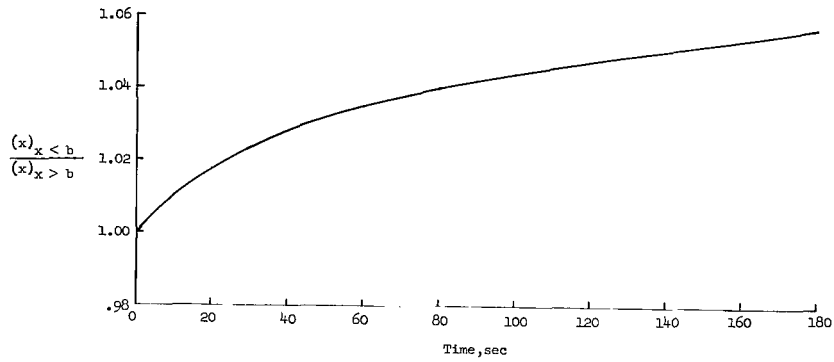
The results of a comparison between the quasi-steady-state exact solution and the numerical analysis are shown in figure 4. For the case considered, the ratio  $\frac{\rho}{\rho' - \rho} = 1$  so that  $\dot{m}_c = \dot{m}_p$ . Figure 4(a) shows the ratio of the mass loss rate obtained from the numerical solution to the value plotted as a function of the distance  $\lambda$  between stations. In the first material, the error is less than 0.7 percent even with large  $\lambda$ .

The ratio of the temperatures obtained from the numerical solution to those obtained from the exact solution plotted as a function of the distance between stations in the first material is shown in figure 4(b) for three locations through the thickness. The error is greatest at the center location, as would be expected, since the temperature is fixed at the surface and interface. Note that the error is less than 0.2 percent even for large  $\lambda$ .

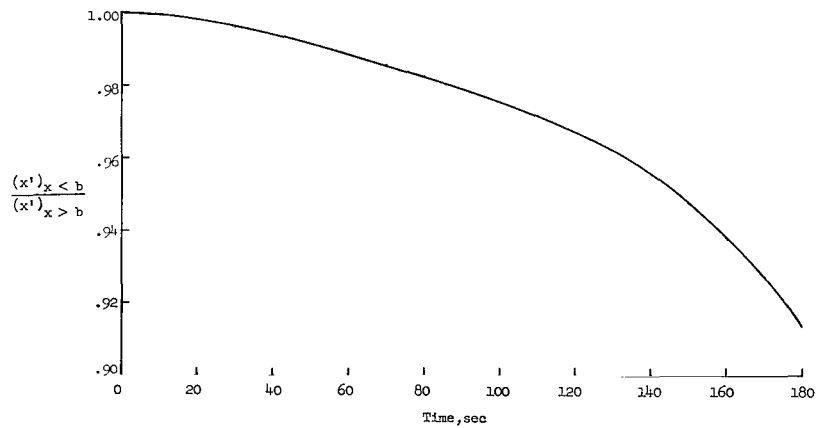
#### Thin-Layer Options

The time interval for which the numerical solution is stable is proportional to the square of the distance between finite-difference stations. (See appendix C.) In general, with the present formulation for the first derivatives, the distance between stations is less than or equal to one-fourth the thickness of the layers. In many cases, the initial value of  $x$ , or the final value of  $x'$ , is very small and excessive computer time is required. To reduce computer time in such cases, equations which eliminate the interior stations when the thickness of a layer is less than a specified value are provided. These equations are derived in appendix C. Specifically, when  $x \leq b$  (referred to as the b-option), the interior stations in the first layer are not considered and the entire layer becomes two half elements of thickness  $x/2$ . If the first layer reaches a reasonable thickness due to pyrolysis at the interface, the thin-layer option is no longer appropriate and the program reverts to the standard equations when this value of  $b$  is exceeded. A b-value, which is one order of magnitude larger than the initial value of  $x$ , generally provides acceptable accuracy and significantly reduces computer time. Similarly, when  $x' \leq b'$  (b'-option), the interior stations of the second layer are discarded. A b'-value, one order of magnitude less than the initial value of  $x'$ , is generally acceptable.

Results obtained with the thin-layer options are compared with the standard solution in figures 5 and 6 for a typical charring ablator subjected to a constant heating rate. The values used in the calculations are given in table III. These values are representative of a low-density phenolic-nylon charring ablator.



(a) Char layer.



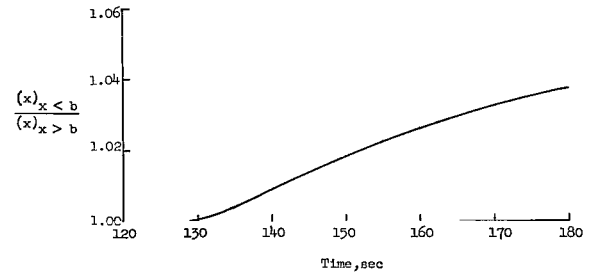
(b) Uncharred layer.

Figure 5.- Error in calculated thickness when thin-char-layer option is used.

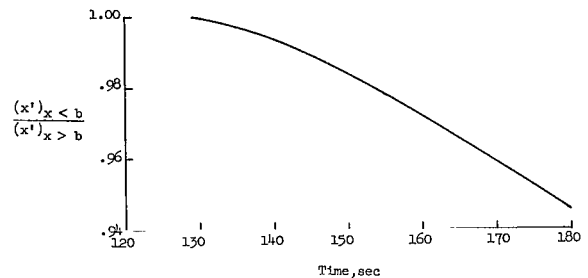
TABLE III.- VALUES USED FOR THIN-LAYER OPTION CALCULATIONS

Quantity	Value in U.S. Customary Units	Value in SI Units
$q_c$ . . . . .	100 Btu/ft <sup>2</sup> -sec	1135 kW/m <sup>2</sup>
$k$ for -		
500° R (278° K) . . . . .	$5 \times 10^{-6}$ Btu/ft <sup>2</sup> -sec-°R	0.0312 W/m-°K
1000° R (556° K) . . . . .	$2 \times 10^{-5}$ Btu/ft <sup>2</sup> -sec-°R	0.1248 W/m-°K
1500° R (834° K) . . . . .	$5 \times 10^{-5}$ Btu/ft <sup>2</sup> -sec-°R	0.312 W/m-°K
2000° R (1110° K) . . . . .	$1.0 \times 10^{-4}$ Btu/ft <sup>2</sup> -sec-°R	0.624 W/m-°K
7000° R (3890° K) . . . . .	$1.0 \times 10^{-3}$ Btu/ft <sup>2</sup> -sec-°R	6.24 W/m-°K
$c_p$ . . . . .	0.5 Btu/lb-°R	2.09 kJ/kg-°K
$\bar{c}_p$ . . . . .	0.5 Btu/lb-°R	2.09 kJ/kg-°K
$c_p^1$ . . . . .	0.32 Btu/lb-°R	1.34 kJ/kg-°K
$k^1$ . . . . .	$3.06 \times 10^{-5}$ Btu/ft-sec-°R	0.191 W/m- $\frac{^\circ K}{ft}$
$\rho$ . . . . .	15 lb/ft <sup>3</sup>	240 kg/m <sup>3</sup>
$\rho^1$ . . . . .	36 lb/ft <sup>3</sup>	576 kg/m <sup>3</sup>
$\Delta h_p$ . . . . .	250 Btu/lb	0.581 MJ/kg
$A$ . . . . .	$6.73 \times 10^8$ lb/ft <sup>2</sup> -sec-atm <sup>1/2</sup>	$3.29 \times 10^9$ kg/m <sup>2</sup> -sec-atm <sup>1/2</sup>
$B$ . . . . .	$3.9877 \times 10^4$ °R	$2.216 \times 10^4$ °K
$C_e$ . . . . .	0.23	
$\lambda$ . . . . .	0.75	
$p_w$ , atm . . . . .	1.3	
$A'$ . . . . .	$1.585 \times 10^6$ lb/ft <sup>2</sup> -sec-atm <sup>1/2</sup>	$7.74 \times 10^6$ kg/m <sup>2</sup> -sec-atm <sup>1/2</sup>
$B'$ . . . . .	$2.321 \times 10^4$ °R	$1.29 \times 10^4$ °K

Figure 5(a) shows the ratio of char-layer thickness using the thin-char-layer option to the char-layer thickness using the standard equations. As can be seen from the figure, when  $x < b$  throughout the calculation, there is an appreciable error. However, for both calculations, the char thickness is monotonically increasing and if a b-value is used such that  $x$  becomes greater than  $b$  during the calculation, the char thickness immediately begins to approach the thickness obtained when the option is not used. Thus, since most of the computer time necessary for a calculation is usually consumed in the beginning of a calculation when the char thickness is small, the use of an intermediate b-value usually produces a considerable saving of computer time without any appreciable error.



(a) Char layer.



(b) Uncharred layer.

Figure 6.- Error in calculated thickness when thin-uncharred-layer option is used.

Figure 5(b) shows the ratio of the thickness of the uncharred layer using the thin-charred-layer option to the uncharred layer thickness using the standard equations. The error which occurs when the b-option is used is significant. However, as with the char layer, the use of an intermediate b-value reduces this error considerably.

Figure 6 shows the results obtained by using the b'-option. The value of  $b'$  used, 0.02 inch (0.05 cm), is such that  $x'$  becomes less than  $b'$  at about 130 seconds. The error shown in the figure can be reduced, if necessary, by using a smaller  $b'$ -value.

#### CONCLUDING REMARKS

Differential equations governing the thermal performance of charring ablaters are derived. These equations are expanded into finite-difference form and have been programed for numerical solution on a digital computer. Numerical results compare favorably with available exact solutions.

The required computer time presents a major problem in the numerical solution of these equations. The governing equations have been examined and a number of approximations which reduce the computer time are introduced. The conditions under which these simplifications should be used and the error involved

in their use are discussed. The computer program based on the equations presented herein has been found to provide a practical basis for heat-shield design studies.

Langley Research Center,  
National Aeronautics and Space Administration,  
Langley Station, Hampton, Va., April 1, 1965.

## APPENDIX A

### EFFECTS OF MASS INJECTION ON AERODYNAMIC HEATING

The aerodynamic heat input consists of both convective heating and radiative heating. The material that is liberated by erosion of the outer surface and pyrolysis at the interface enters the boundary layer and causes a significant reduction in convective heating. It has been shown (refs. 20, 21, and 22) that, for moderate mass-transfer rates, the effectiveness of mass transfer in blocking convective heating is approximately a linear function of the enthalpy in the flow outside the boundary layer. It is further shown in references 22 and 23, however, that this approximation may lead to serious error if the surface is exposed to a net radiant heat input such as that which a typical vehicle would experience from reentry at parabolic or hyperbolic velocities.

Blocking effectiveness as a function of a mass-transfer-rate parameter  $\dot{m}h_e/q_C$  (where  $\dot{m} = \alpha_c \dot{m}_c + \alpha_p \dot{m}_p$ ) is shown in figure 7. The exact solution was obtained from the boundary-layer solutions for air-to-air injection (ref. 21). It can be seen from figure 7 that the usual linear approximation for a laminar boundary layer is not valid at higher values of the mass-transfer-rate parameter. The effect of radiant heating is to increase  $\dot{m}$  and this increase results in operation at higher values of  $\dot{m}h_e/q_C$ . The second-degree approximation was developed by fitting a curve at values of  $\dot{m}h_e/q_C$  of 0, 1.0, and 2.5.

Very little experimental data is available at high mass-transfer rates, and in conservative calculations it is desirable to specify a minimum value of

$$\frac{q_{C,net}}{q_C \left(1 - \frac{h_w}{h_e}\right)} \text{ greater than } 0.$$

This approach is certainly in order if boundary-layer separation is found to occur at high mass-injection rates. In this analysis, a minimum value of the q-ratio (0.04) was specified where the second-degree approximation departs from the theoretical curve.

The equation for the second-degree approximation is as follows:

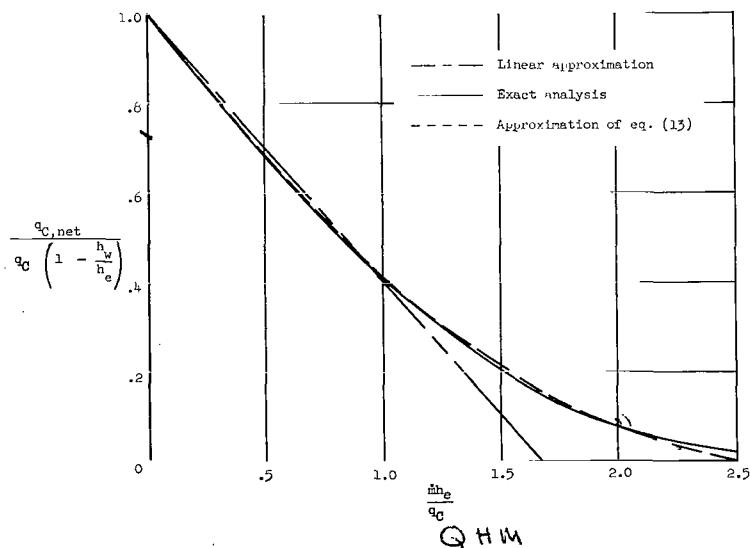


Figure 7.- Blocking effectiveness for a laminar boundary layer with air-to-air injection.

APPENDIX A

$$\left. \begin{aligned} \frac{q_{C,net}}{q_C \left(1 - \frac{h_w}{h_e}\right)} &= 1 - 0.724 \frac{h_e}{q_C} (\alpha_c \dot{m}_c + \alpha_p \dot{m}_p) + 0.13 \left(\frac{h_e}{q_C}\right)^2 (\alpha_c \dot{m}_c + \alpha_p \dot{m}_p)^2; & \left(\frac{h_e}{q_C} (\alpha_c \dot{m}_c + \alpha_p \dot{m}_p) < 2.25\right) \\ \frac{q_{C,net}}{q_C \left(1 - \frac{h_w}{h_e}\right)} &= 0.04; & \left(\frac{h_e}{q_C} (\alpha_c \dot{m}_c + \alpha_p \dot{m}_p) \geq 2.25\right) \end{aligned} \right\} \quad (A1)$$

The constants  $\alpha_c$  and  $\alpha_p$  are used to correct equation (A1) for the difference between the molecular weight of the boundary-layer gas and the molecular weight of the injected gas. The constant  $\alpha_c$  must also be corrected for that part of the char that is removed mechanically, that is, for the char that is removed but not sublimed. A similar approach might be used to correct for turbulent flow. The effects of molecular weight and turbulent flow are discussed in reference 24. An equation of the form of equation (A1) is used to correlate experimental data in reference 18 by using the correction of reference 24 for molecular weight effects. The equations have been formulated to provide the option of using either the linear function of enthalpy (ablation theory) or a second-degree approximation to the actual blocking effectiveness (transpiration theory).

## APPENDIX B

### FINITE-DIFFERENCE EQUATIONS

The system of partial differential equations to be solved is extremely complicated (nonlinear with variable coefficients) and solutions in analytic form can hardly be expected. The systems can be put into a form suitable for numerical calculation by deriving the equations in finite-difference form and then solving them by an iteration procedure on a high-speed digital computer.

For this type of procedure it is convenient to space the finite-difference stations at equal intervals throughout a given layer, as shown in figure 2. The first (char) layer contains  $i$  stations including one at the front and one at the back surface of the first layer. The second layer contains  $j$  stations including one at the back surface of the second layer. The third layer (if desired) contains  $m$  stations including one at the back surface.

The distances between stations are therefore

$$\left. \begin{aligned} \lambda &= \frac{x}{i-1} \\ \lambda' &= \frac{x'}{j} \\ \lambda'' &= \frac{x''}{m} \end{aligned} \right\} \quad (B1)$$

for the three layers whose thicknesses are  $x$ ,  $x'$ , and  $x''$ , respectively. In this appendix, the finite-difference form of the general equations (eqs. (24a), (24b), and (3)) are presented first and then the finite-difference form of the boundary equations (eqs. (25a), (26b), (27), and (29)) are given.

#### Interior Stations

Char layer ( $2 \leq n \leq i-1$ ).— The finite-difference form of equation (24a)

$$\frac{1}{x^2} \frac{\partial}{\partial \xi} \left( k \frac{\partial \theta}{\partial \xi} \right) + \frac{1}{x} \frac{\partial \theta}{\partial \xi} \left[ \dot{m}_c c_p + \dot{m}_p \bar{c}_p + \xi \left( \frac{\dot{m}_p \rho}{\rho' - \rho} - \dot{m}_c \right) c_p \right] + F = \rho c_p \frac{\partial \theta}{\partial t} \quad (B2)$$

is obtained as follows: The second derivative (first term of eq. (B2)) is obtained by a Taylor series expansion at station  $n$  evaluated at the points  $\left(n - \frac{1}{2}\right)$  and  $\left(n + \frac{1}{2}\right)$ . Thus,

APPENDIX B

$$\left. \begin{aligned} k\left(\frac{\partial\theta}{\partial\xi}\right)_{n-\frac{1}{2}} &= k\left(\frac{\partial\theta}{\partial\xi}\right)_n - \frac{\Delta\xi}{2} \frac{\partial}{\partial\xi} \left(k \frac{\partial\theta}{\partial\xi}\right)_n + \frac{(\Delta\xi)^2}{8} \frac{\partial^2}{\partial\xi^2} \left(k \frac{\partial\theta}{\partial\xi}\right)_n - \frac{(\Delta\xi)^3}{48} \frac{\partial^3}{\partial\xi^3} \left(k \frac{\partial\theta}{\partial\xi}\right)_n \\ k\left(\frac{\partial\theta}{\partial\xi}\right)_{n+\frac{1}{2}} &= k\left(\frac{\partial\theta}{\partial\xi}\right)_n + \frac{\Delta\xi}{2} \frac{\partial}{\partial\xi} \left(k \frac{\partial\theta}{\partial\xi}\right)_n + \frac{(\Delta\xi)^2}{8} \frac{\partial^2}{\partial\xi^2} \left(k \frac{\partial\theta}{\partial\xi}\right)_n + \frac{(\Delta\xi)^3}{48} \frac{\partial^3}{\partial\xi^3} \left(k \frac{\partial\theta}{\partial\xi}\right)_n \end{aligned} \right\} \quad (B3)$$

These equations are then solved for the second derivative and yield

$$\frac{1}{x} \frac{\partial}{\partial\xi} \left(k \frac{\partial\theta}{\partial\xi}\right)_n = \frac{1}{l} \left(k \frac{\partial\theta}{\partial\xi}\right)_{n+\frac{1}{2}} - \frac{1}{l} \left(k \frac{\partial\theta}{\partial\xi}\right)_{n-\frac{1}{2}} + \frac{(\Delta\xi)^2}{24x} \frac{\partial^3}{\partial\xi^3} \left(k \frac{\partial\theta}{\partial\xi}\right)_n \quad (B4)$$

or

$$\frac{1}{x^2} \frac{\partial}{\partial\xi} \left(k \frac{\partial\theta}{\partial\xi}\right)_n \approx \frac{1}{l} \left(k_{n,n+1} \frac{T_{n+1} - T_n}{l} - k_{n-1,n} \frac{T_n - T_{n-1}}{l}\right)$$

which is correct to order  $l^2$ . Note that  $x \Delta\xi = l$ .

The finite-difference form of the first partial derivative in the second term of equation (B2) is obtained by a Taylor series expansion about station  $n$  evaluated at  $n-1$ ,  $n+1$ , and  $n+2$ . Thus

$$\left. \begin{aligned} \theta_{n-1} &= \theta_n - \Delta\xi \left(\frac{\partial\theta}{\partial\xi}\right)_n + \frac{(\Delta\xi)^2}{2} \left(\frac{\partial^2\theta}{\partial\xi^2}\right)_n - \frac{(\Delta\xi)^3}{6} \left(\frac{\partial^3\theta}{\partial\xi^3}\right)_n + \frac{(\Delta\xi)^4}{24} \left(\frac{\partial^4\theta}{\partial\xi^4}\right)_n - \dots \\ \theta_{n+1} &= \theta_n + \Delta\xi \left(\frac{\partial\theta}{\partial\xi}\right)_n + \frac{(\Delta\xi)^2}{2} \left(\frac{\partial^2\theta}{\partial\xi^2}\right)_n + \frac{(\Delta\xi)^3}{6} \left(\frac{\partial^3\theta}{\partial\xi^3}\right)_n + \frac{(\Delta\xi)^4}{24} \left(\frac{\partial^4\theta}{\partial\xi^4}\right)_n + \dots \\ \theta_{n+2} &= \theta_n + 2\Delta\xi \left(\frac{\partial\theta}{\partial\xi}\right)_n + \frac{(2\Delta\xi)^2}{2} \left(\frac{\partial^2\theta}{\partial\xi^2}\right)_n + \frac{(2\Delta\xi)^3}{6} \left(\frac{\partial^3\theta}{\partial\xi^3}\right)_n \\ &\quad + \frac{(2\Delta\xi)^4}{24} \left(\frac{\partial^4\theta}{\partial\xi^4}\right)_n + \dots \end{aligned} \right\} \quad (B5)$$

APPENDIX B

This set of equations is solved for the first derivative and yields

$$\frac{1}{x} \frac{\partial \theta}{\partial \xi} = \frac{1}{6l} (6T_{n+1} - 3T_n - 2T_{n-1} - T_{n+2}) + \frac{(\Delta \xi)^3}{12} \left( \frac{\partial^4 \theta}{\partial \xi^4} \right)_n \quad (B6)$$

Therefore, the expression

$$\frac{1}{6l} (6T_{n+1} - 3T_n - 2T_{n-1} - T_{n+2}) \quad (B7)$$

is an approximate derivative at station  $n$  ( $2 \leq n \leq i - 2$ ) correct to terms of order  $l^3$ .

At station  $n = i - 1$ , the series is evaluated at  $n - 2$ ,  $n - 1$ , and  $n + 1$  since there is a discontinuity at station  $i$ . This procedure gives

$$\frac{1}{x} \left( \frac{\partial \theta}{\partial \xi} \right)_{i-1} = \frac{1}{6l} (2T_i + 3T_{i-1} - 6T_{i-2} + T_{i-3}) \quad (B8)$$

which is also correct to terms of order  $l^3$ .

Substituting equations (B4) and (B7) into equation (B2) gives the finite-difference form of equation (B2) as

$$\begin{aligned} & k_{n-1,n} \frac{T_{n-1} - T_n}{l} - k_{n,n+1} \frac{T_n - T_{n+1}}{l} \\ & + \frac{1}{6} (6T_{n+1} - 3T_n - 2T_{n-1} - T_{n+2}) \left[ \dot{m}_c c_p + \dot{m}_p \bar{c}_p + \frac{n-1}{i-1} \left( \frac{\dot{m}_p \rho}{\rho' - \rho} - \dot{m}_c \right) c_p \right] \\ & + lF = \rho c_p l \frac{\Delta T_n}{\Delta t} \quad (2 \leq n \leq i - 2) \quad (B9) \end{aligned}$$

and by using equation (B8) instead of equation (B7), the equation is

$$\begin{aligned} & k_{n-1,n} \frac{T_{n-1} - T_n}{l} - k_{n,n+1} \frac{T_n - T_{n+1}}{l} \\ & + \frac{1}{6} (2T_{n+1} + 3T_n - 6T_{n-1} + T_{n-2}) \left[ \dot{m}_c c_p + \dot{m}_p \bar{c}_p + \frac{n-1}{i-1} \left( \frac{\dot{m}_p \rho}{\rho' - \rho} - \dot{m}_c \right) c_p \right] \\ & + lF = \rho c_p l \frac{\Delta T_n}{\Delta t} \quad (n = i - 1) \quad (B10) \end{aligned}$$

APPENDIX B

Uncharred material ( $i + 1 \leq n \leq i + j - 1$ ).— The transformed equation for the second layer (eq. (24b)) is

$$\frac{1}{(x')^2} \frac{\partial}{\partial \zeta} \left( k' \frac{\partial \theta'}{\partial \zeta} \right) + \frac{1}{x'} \frac{\dot{m}_p \rho' c_p'}{\rho' - \rho} (1 - \zeta) \frac{\partial \theta'}{\partial \zeta} = \rho' c_p' \frac{\partial \theta'}{\partial t} \quad (B11)$$

The second partial derivative is found as in the previous section and is given by the following finite-difference expression (correct to order  $\lambda^2$ ).

$$\frac{1}{(x')^2} \frac{\partial}{\partial \zeta} \left( k' \frac{\partial \theta}{\partial \zeta} \right)_n = \frac{1}{\lambda'} \left( k'_{n-1,n} \frac{T_{n-1} - T_n}{\lambda'} - k'_{n,n+1} \frac{T_n - T_{n+1}}{\lambda'} \right) \quad (B12)$$

and as in the previous section, the first derivative is obtained by a Taylor series expansion about station  $n$

$$\left( \frac{1}{x'} \frac{\partial \theta}{\partial \zeta} \right)_n = \frac{1}{6\lambda'} (6T_{n+1} - 3T_n - 2T_{n-1} - T_{n+2}) \quad (i + 1 \geq n \geq i + j - 2) \quad (B13)$$

and

$$\left( \frac{1}{x'} \frac{\partial \theta}{\partial \zeta} \right)_{i+j-1} = \frac{1}{6\lambda'} (2T_{n+1} + 3T_n - 6T_{n-1} + T_{n-2}) \quad (n = i + j - 1) \quad (B14)$$

These expressions are again correct to order  $\lambda^3$ .

This procedure gives the finite-difference form of equation (B11) as

$$\begin{aligned} & k'_{n-1,n} \frac{T_{n-1} - T_n}{\lambda'} - k'_{n,n+1} \frac{T_n - T_{n+1}}{\lambda'} \\ & + \frac{1}{6} (6T_{n+1} - 3T_n - 2T_{n-1} - T_{n+2}) \frac{i + j - n}{j} \frac{\dot{m}_p \rho' c_p'}{\rho' - \rho} = \rho' c_p' \lambda' \frac{\Delta T_n}{\Delta t} \end{aligned} \quad (i + 1 \leq n \leq i + j - 2) \quad (B15)$$

APPENDIX B

and as

$$k'_{n-1,n} \frac{T_{n-1} - T_n}{\lambda'} - k'_{n,n+1} \frac{T_n - T_{n+1}}{\lambda'}$$

$$+ \frac{1}{6} (2T_{n+1} + 3T_n - 6T_{n-1} + T_{n-2}) \frac{i + j - n}{j} \frac{\dot{m}_p \rho' c'_p}{\rho' - \rho} = \lambda' \rho' c'_p \frac{\Delta T_n}{\Delta t}$$

(n = i + j - 1) (B16)

Insulation (i + j + 1 ≤ n ≤ i + j + m - 1). - The differential equation for the third layer is (eq. (3))

$$\frac{\partial}{\partial y} \left( k'' \frac{\partial \theta''}{\partial y} \right) = \rho'' c''_p \frac{\partial \theta''}{\partial t}$$

(B17)

The second derivative is given by the expression (correct to order  $\lambda^2$ )

$$\frac{\partial}{\partial y} \left( k'' \frac{\partial \theta''}{\partial y} \right)_n = k''_{n-1,n} \frac{T_{n-1} - T_n}{\lambda''} - k''_{n,n-1} \frac{T_n - T_{n+1}}{\lambda''}$$

(B18)

Therefore, the difference equation is,

$$k''_{n-1,n} \frac{T_{n-1} - T_n}{\lambda''} - k''_{n,n+1} \frac{T_n - T_{n+1}}{\lambda''} = \lambda'' \rho'' c''_p \frac{\Delta T_n}{\Delta t}$$

(B19)

Boundary Stations

First station (ξ = 0). - Some difficulty is encountered in finding an acceptable finite-difference equation for the first station. The first approach that is used to obtain such an equation is relatively straightforward. First, the second partial derivative of equation (B2) is expanded in a Taylor series about the point ξ = 0 and evaluated at ξ =  $\frac{\Delta \xi}{2}$ .

$$\frac{1}{x^2} \frac{\partial}{\partial \xi} \left( k \frac{\partial \theta}{\partial \xi} \right)_{\xi=0} = \frac{2}{\lambda} \left[ k_{1,2} \frac{T_2 - T_1}{\lambda} - \frac{1}{x} \left( k \frac{\partial \theta}{\partial \xi} \right)_{\xi=0} \right]$$

(B20)

APPENDIX B

Substituting equation (B20) into equation (B2) gives

$$\frac{2}{l} \left[ k_{1,2} \frac{T_2 - T_1}{l} - \frac{1}{x} \left( k \frac{\partial \theta}{\partial \xi} \right)_{\xi=0} \right] + \frac{1}{x} \left( \frac{\partial \theta}{\partial \xi} \right)_{\xi=0} (\dot{m}_c c_p + \dot{m}_p \bar{c}_p) + F = \rho c_p \frac{\Delta T_1}{\Delta t} \quad (B21)$$

The transformed equation for the boundary condition at the first station (eq. (25a)) is

$$q_{aero} = \sigma \epsilon_1 \theta^4 - \frac{k}{x} \frac{\partial \theta}{\partial \xi} + \dot{m}_c \left[ S(\theta - \bar{T}_1)(H_c + \Delta h_c) - \Delta h_c \right] \quad (B22)$$

where  $q_{aero}$  is given by equation (25b).

The exact value of  $\left( \frac{1}{x} \frac{\partial \theta}{\partial \xi} \right)_{\xi=0}$  from equation (B22) is then substituted into equation (B21) to yield

$$k_{1,2} \frac{T_2 - T_1}{l} - \left\{ \sigma \epsilon_1 T_1^4 + \dot{m}_c \left[ S(\theta - \bar{T}_1)(H_c + \Delta h_c) - \Delta h_c \right] - q_{aero} \right\} \left[ 1 - \frac{l}{2k} (\dot{m}_c c_p + \dot{m}_p \bar{c}_p) \right] + \frac{l}{2} F = \rho c_p \frac{l}{2} \frac{\Delta T_1}{\Delta t} \quad (B23)$$

The difficulty encountered in attempting to use this equation is due to the term  $1 - \frac{l}{2k} (\dot{m}_c c_p + \dot{m}_p \bar{c}_p)$ . This term must be approximately equal to 1 since  $l$  is an approximation to an infinitesimal. However, since  $k$  is typically of the order  $10^{-4}$  or smaller,  $l$  must be taken so small that the computer time required for an acceptable solution is unreasonable.

To alleviate this problem, a different expression for the second first derivative of equation (B21) is used. This expression was found by expanding the temperature at station 1 in a Taylor series evaluated at stations 2, 3, and 4 which gives

$$\frac{1}{x} \left( \frac{\partial \theta}{\partial \xi} \right)_{\xi=0} = \frac{1}{6l} (-11T_1 + 18T_2 - 9T_3 + 2T_4) \quad (B24)$$

APPENDIX B

Hence the finite-difference equation for station 1 becomes

$$k_{1,2} \frac{T_2 - T_1}{l} + q_{aero} - \sigma \epsilon_1 T_1^4 - \dot{m}_c \left[ S(T_1 - \bar{T}_1)(H_c + \Delta h_c) - \Delta h_c \right] + \frac{1}{12} (-11T_1 + 18T_2 - 9T_3 + 2T_4) (\dot{m}_c c_p + \dot{m}_p \bar{c}_p) + \frac{l}{2} F = \rho c_p \frac{l}{2} \frac{\Delta T_1}{\Delta t} \quad (B25)$$

Note that the exact expression for  $\left( \frac{1}{x} \frac{\partial \theta}{\partial \xi} \right)_{\xi=0}$  from equation (B22) is still used for the first first derivative.

Interface ( $\xi = 1, \zeta = 0$ ). - The transformed equation at the interface boundary  $\xi = 1, \zeta = 0$  is (eq. (26b))

$$-\left( \frac{k}{x} \frac{\partial \theta}{\partial \xi} \right)_{\xi=1} = \dot{m}_p \Delta h_p - \left( \frac{k'}{x'} \frac{\partial \theta'}{\partial \zeta} \right)_{\zeta=0} \quad (B26)$$

The finite-difference form of equation (B27) is found by a simultaneous solution of equations (B2) at  $\xi = 1$ , (B11) at  $\zeta = 0$ , and (B26). In this way, the interface equation is satisfied both at the interface and also immediately on either side of the interface. To do this, equation (B21) is rewritten for  $\xi = 1$ . Thus,

$$-\left( \frac{k}{x} \frac{\partial \theta}{\partial \xi} \right)_{\xi=1} = -k_{i-1,i} \frac{T_i - T_{i-1}}{l} + \frac{l}{\Delta x} \left( \frac{\partial \theta}{\partial \xi} \right)_{\xi=1} \dot{m}_p \left( \bar{c}_p + \frac{c_{p\rho}}{\rho' - \rho} \right) + \frac{l}{2} F - \rho c_p \frac{l}{2} \frac{\Delta T_i}{\Delta t} \quad (B27)$$

Then by using a Taylor's series expansion about station  $i$ , evaluated at  $i - 1$ ,  $i - 2$ , and  $i - 3$ , equation (B28) can be written as

$$-\left( \frac{k}{x} \frac{\partial \theta}{\partial \xi} \right)_{\xi=1} = -k_{i-1,i} \frac{T_i - T_{i-1}}{l} + \frac{\dot{m}_p}{12} \left( \bar{c}_p + \frac{c_{p\rho}}{\rho' - \rho} \right) (11T_i - 18T_{i-1} + 9T_{i-2} - 2T_{i-3}) + \frac{l}{2} F - \rho c_p \frac{l}{2} \frac{\Delta T_i}{\Delta t} \quad (B28)$$

APPENDIX B

A similar procedure using equation (B11) at  $\zeta = 0$  gives

$$\begin{aligned} -\left(\frac{k'}{x'} \frac{\partial \theta'}{\partial \zeta}\right)_{\zeta=0} &= -k'_{i,i+1} \frac{T_{i+1} - T_i}{\lambda'} - \frac{\dot{m}_p}{12} \left(\frac{c'_p \rho'}{\rho' - \rho}\right) (-11T_i + 18T_{i+1} \\ &\quad - 9T_{i+2} + 2T_{i+3}) + \rho' c'_p \frac{\lambda'}{2} \frac{\Delta T_i}{\Delta t} \end{aligned} \quad (B29)$$

Finally, substitution of equations (B28) and (B29) into equation (B26) gives

$$\begin{aligned} k'_{i,i+1} \frac{T_{i+1} - T_i}{\lambda'} - k'_{i-1,i} \frac{T_i - T_{i-1}}{\lambda} + \dot{m}_p \left\{ \left( \bar{c}_p + \frac{\rho c_p}{\rho' - \rho} \right) \left[ \frac{1}{12} (11T_i - 18T_{i-1} \right. \right. \\ \left. \left. + 9T_{i-2} - 2T_{i-3}) \right] + \frac{c'_p \rho'}{\rho' - \rho} \left[ \frac{1}{12} (-11T_i + 18T_{i+1} - 9T_{i+2} + 2T_{i+3}) \right] - \Delta h_p \right\} \\ + \frac{\lambda}{2} F = \left( \rho c_p \frac{\lambda}{2} + \rho' c'_p \frac{\lambda'}{2} \right) \frac{\Delta T_i}{\Delta t} \end{aligned} \quad (B30)$$

Back surface (2 layers,  $\zeta = 1$ ). - For a two-layer system, the transformed boundary equation is (eq. (27))

$$\begin{aligned} -\frac{k'}{x'} \left( \frac{\partial \theta'}{\partial \zeta} \right)_{\zeta=1} &= C_{i+j} \frac{\partial \theta'}{\partial t} + S (\theta' - \bar{T}_{i+j}) \Delta W_F \Delta h_F \\ &\quad + \sigma \epsilon_{i+j} \left[ (\theta')^4 - T_B^4 \right] \end{aligned} \quad (B31)$$

The first term of equation (B31) is determined by evaluating equation (B11) at  $\zeta = 1$ ; thus,

$$-\left(\frac{k'}{x'} \frac{\partial \theta'}{\partial \zeta}\right)_{\zeta=1} = -k'_{i+j-1,i+j} \frac{T_{i+j} - T_{i+j-1}}{\lambda'} - \rho' c'_p \frac{\lambda'}{2} \frac{\Delta T_{i+j}}{\Delta t} \quad (B32)$$

Substituting equation (B32) into equation (B31) gives

$$\begin{aligned} k'_{i+j-1,i+j} \frac{T_{i+j-1} - T_{i+j}}{\lambda'} - \sigma \epsilon_{i+j} (T_{i+j}^4 - T_B^4) \\ - S (T_{i+j} - \bar{T}_{i+j}) \Delta W_F \Delta h_F = \left( \rho' c'_p \frac{\lambda'}{2} + C_{i+j} \right) \frac{\Delta T_{i+j}}{\Delta t} \end{aligned} \quad (B33)$$

APPENDIX B

Interface (3 layers,  $\xi = 1$ ).- For a three-layer system, the transformed boundary equation at  $\xi = 1$  is (eq. (28b))

$$-\left(\frac{k'}{x'} \frac{\partial \theta'}{\partial \xi}\right)_{\xi=1} = C_{i+j} \frac{\partial \theta'}{\partial t} - \left(k'' \frac{\partial \theta''}{\partial y}\right)_{y=x_0+x_0'} \quad (B34)$$

The first term of equation (B34) is given by equation (B32). The last term of equation (B34) is evaluated by expanding the second derivative of equation (B18). Thus,

$$-\left(k'' \frac{\partial \theta''}{\partial y}\right)_{x_0+x_0'} = -k''_{i+j, i+j+1} \frac{T_{i+j+1} - T_{i+j}}{l''} + \rho'' c_p'' \frac{l''}{2} \frac{\Delta T_{i+j}}{\Delta t} \quad (B35)$$

Substituting equations (B32) and (B35) into equation (B34) gives

$$k'_{i+j-1, i+j} \frac{T_{i+j-1} - T_{i+j}}{l'} - k''_{i+j, i+j+1} \frac{T_{i+j} - T_{i+j+1}}{l''} = \left(\rho' c_p' \frac{l'}{2} + \rho'' c_p'' \frac{l''}{2} + C_{i+j}\right) \frac{\Delta T_{i+j}}{\Delta t} \quad (B36)$$

Back surface (3 layers,  $n = i + j + m$ ).- For a three-layer system, the back-surface boundary condition is (eq. (29))

$$-k'' \frac{\partial \theta''}{\partial y} = C_{i+j+m} \frac{\partial \theta''}{\partial t} + S(\theta'' - \bar{T}_{i+j+m}) \Delta W_f \Delta h_f + \sigma \epsilon_{i+j+m} \left[ (\theta'')^4 - T_B^4 \right] \quad (B37)$$

Equation (B37) is solved simultaneously with equation (B17), with the previously used approximation to the second derivative, to yield,

$$k''_{i+j+m-1, i+j+m} \frac{T_{i+j+m-1} - T_{i+j+m}}{l''} = \sigma \epsilon_{i+j+m} (T_{i+j+m}^4 - T_B^4) + S(T_{i+j+m} - \bar{T}_{i+j+m}) \Delta W_f \Delta h_f + \left(\rho'' c_p'' \frac{l''}{2} + C_{i+j+m}\right) \frac{\Delta T_{i+j+m}}{\Delta t} \quad (B38)$$

## APPENDIX C

### SIMPLIFICATIONS TO REDUCE COMPUTING TIME

#### Computing the Time Interval

The primary difficulty encountered in using the program is the time required to obtain solutions on the digital computer. The equations are integrated stepwise over time, and the maximum time interval for which the solution is stable with the explicit formulation used is (ref. 25),

$$\Delta t = \frac{\rho c_p l^2}{2k}$$

where the properties of the layer giving the minimum  $\Delta t$  must be used.

Theoretically, the initial value of  $l$  may be zero in the physical sense; however, a finite initial char thickness is required for the calculating procedure used in this program. The initial value of the char thickness which is usually chosen is extremely small. As the thickness of the char layer increases due to the pyrolysis at the interface, the preceding stability equation allows the digital computer to use a larger time interval in its stepwise calculations. Likewise, when the second material pyrolyzes to such an extent that its  $l$  becomes very small, the preceding equation now decreases the time interval so that the finite-difference equations remain stable. This time interval is only allowed to change whenever the digital computer can recognize this change and continue to print out answers at the specified print-out times. Also the computer recognizes specified minimum values for both  $x$  and  $x'$  so that computer time is not wasted when either  $x$  or  $x'$  approaches zero.

#### Options for Thin-Layer Configurations

In some cases, it is necessary to run calculations where the stability time interval  $\Delta t$  becomes very small. Therefore, to decrease computing time by at least one-half, the computer recognizes input quantities  $b$  and  $b'$ . When  $x \leq b$  and/or  $x' \leq b'$ , the interior stations are no longer considered and the entire layer becomes two half elements of thickness  $x/2$  and/or  $x'/2$ . In this procedure the following finite-difference equations are utilized.

When  $x \leq b$ , the equations at the first station (eq. (B25)) become

$$2k_{1,i} \frac{T_i - T_1}{x} + 2 \left\{ q_{aero} - \sigma \epsilon_1 T_1^4 - \dot{m}_c \left[ S(T_1 - \bar{T}_1)(H_c + \Delta h_c) - \Delta h_c \right] \right\} + (T_i - T_1)(\dot{m}_c c_p + \dot{m}_p \bar{c}_p) + xF = \rho c_p x \frac{\Delta T_1}{\Delta t} \quad (C1)$$

APPENDIX C

The equations for the interior stations in the char layer are no longer considered when  $x \leq b$ . The equation at the interface (eqs. (B30)) is as follows:

When  $x \leq b$  and  $x' > b'$

$$2k'_{i,i+1} \frac{T_{i+1} - T_i}{l'} - 2k_{1,i} \frac{T_i - T_1}{x} + xF + \dot{m}_p \left\{ \left( \bar{c}_p + \frac{\rho c_p}{\rho' - \rho} \right) (T_i - T_1) + \frac{c'_p \rho'}{\rho' - \rho} \left[ \frac{1}{6} (-11T_i + 18T_{i+1} - 9T_{i+2} + 2T_{i+3}) \right] - 2\Delta h_p \right\} = (\rho c_p x + \rho' c'_p l') \frac{\Delta T_i}{\Delta t} \quad (C2)$$

When  $x \leq b$  and  $x' \leq b'$

$$2k'_{i,i+j} \frac{T_{i+j} - T_i}{x'} - 2k_{1,i} \frac{T_i - T_1}{x} + xF + \dot{m}_p \left\{ \left( \bar{c}_p + \frac{\rho c_p}{\rho' - \rho} \right) (T_i - T_1) + \frac{c'_p \rho'}{\rho' - \rho} (T_{i+j} - T_i) - 2\Delta h_p \right\} = (\rho c_p x + \rho' c'_p x') \frac{\Delta T_i}{\Delta t} \quad (C3)$$

When  $x > b$  and  $x' \leq b'$

$$2k'_{i,i+j} \frac{T_{i+j} - T_i}{x'} - 2k_{i-1,i} \frac{T_i - T_{i-1}}{l} + lF + \dot{m}_p \left\{ \left( \bar{c}_p + \frac{\rho c_p}{\rho' - \rho} \right) \left[ \frac{1}{6} (11T_i - 18T_{i-1} + 9T_{i-2} - 2T_{i-3}) \right] + \frac{c'_p \rho'}{\rho' - \rho} (T_{i+j} - T_i) - 2\Delta h_p \right\} = (\rho c_p l + \rho' c'_p x') \frac{\Delta T_i}{\Delta t} \quad (C4)$$

When  $x' \leq b'$ , the interior stations in the second layer are not considered. The equations at the back of the second layer (eq. (B33)) for two layers, (eq. (B38) for three layers) are as follows:

When  $x \leq b'$ , equation (B33) becomes

$$k'_{i,i+j} \frac{T_i - T_{i+j}}{x'} - \sigma \epsilon_{i+j} (T_{i+j}^h - T_B^h) - S (T_{i+j} - \bar{T}_{i+j}) \Delta W_f \Delta h_f = \left( \rho' c'_p \frac{x'}{2} + c_{i+j} \right) \frac{\Delta T_{i+j}}{\Delta t} \quad (C5)$$

APPENDIX C

and equation (B38) becomes

$$k'_{i,i+j} \frac{T_i - T_{i+j}}{x'} - k''_{i+j,i+j+1} \frac{T_{i+j} - T_{i+j+1}}{z''} = \left( \rho' c'_p \frac{x'}{2} + \rho'' c''_p \frac{z''}{2} + C_{i+j} \right) \frac{\Delta T_{i+j}}{\Delta t} \quad (C6)$$

The computer uses the standard equations whenever  $x > b$ , and/or  $x' > b'$ .

## REFERENCES

1. Swann, Robert T.: Composite Thermal Protection Systems for Manned Re-Entry Vehicles. ARS Jour., vol. 32, no. 2, Feb. 1962, pp. 221-226.
2. Chapman, Andrew J.: Effect of Weight, Density, and Heat Load on Thermal-Shielding Performance of Phenolic Nylon. NASA TN D-2196, 1964.
3. Farmer, Rex W.: Ablative Behavior of Plastics in Subsonic and Supersonic Hyperthermal Flow. WADD Tech. Rept. 60-648, U.S. Air Force, Nov. 1960.
4. Schwartz, H. S. [compiler]: Conference on Behavior of Plastics in Advanced Flight Vehicle Environments. WADD Tech. Rep. 60-101, U.S. Air Force, Sept. 1960.
5. Brooks, William A., Jr.; Wadlin, Kenneth L.; Swann, Robert T.; and Peters, Roger W.: An Evaluation of Thermal Protection for Apollo. NASA TM X-613, 1961.
6. Schmidt, Donald L.: Behavior of Plastic Materials in Hyperthermal Environments. WADC Tech. Rep. 59-574, U.S. Air Force, Apr. 1960.
7. Munson, T. R.; and Spindler, R. J.: Transient Thermal Behaviour of Decomposing Materials. Part I: General Theory and Application to Convective Heating. Paper No. 62-30, S.M.F. Publ. Fund, Inst. Aerospace Sci., Jan. 1962.
8. Kratsch, K. M.; Hearne, L. F.; and McChesney, H. R.: Thermal Performance of Heat Shield Composites During Planetary Entry. Presented at AIAA-NASA National Meeting (Palo Alto, Calif.), Sept. 30-Oct. 1, 1963.
9. Swann, Robert T.; and Pittman, Claud M.: Numerical Analysis of the Transient Response of Advanced Thermal Protection Systems for Atmospheric Entry. NASA TN D-1370, 1962.
10. Beecher, Norman; and Rosensweig, Ronald E.: Ablation Mechanisms in Plastics With Inorganic Reinforcement. ARS J., vol. 31, no. 4, Apr. 1961, pp. 532-539.
11. Dow, Marvin B.; and Swann, Robert T.: Determination of Effects of Oxidation on Performance of Charring Ablators. NASA TR R-196, 1964.
12. Scala, Sinclair M.; and Gilbert, Leon M.: Thermal Degradation of a Char-Forming Plastic During Hypersonic Flight. ARS Jour., vol. 32, no. 6, June 1962, pp. 917-924.
13. Mechtly, E. A.: The International System of Units - Physical Constants and Conversion Factors. NASA SP-7012, 1964.

14. Nolan, Edward J.; and Scala, Sinclair M.: Aerothermodynamic Behavior of Pyrolytic Graphite During Sustained Hypersonic Flight. ARS Jour., vol. 32, no. 1, Jan. 1962, pp. 26-35.
15. Truitt, Robert Wesley: Hypersonic Aerodynamics. The Ronald Press Co., c.1959.
16. Chapman, Dean R.: An Approximate Analytical Method for Studying Entry Into Planetary Atmospheres. NASA TR R-11, 1959. (Supersedes NACA TN 4276.)
17. Swann, Robert T.: Approximate Analysis of the Performance of Char-Forming Ablators. NASA TR R-195, 1964.
- ✓ 18. Vojvodich, Nick S.; and Pope, Ronald B.: Effect of Gas Composition on the Ablation Behavior of a Charring Material. AIAA J., vol. 2, no. 3, Mar. 1964, pp. 536-542.
19. Brooks, William A., Jr.: Temperature and Thermal-Stress Distributions in Some Structural Elements Heated at a Constant Rate. NACA TN 4306, 1958.
- \* 20. Roberts, Leonard: Mass Transfer Cooling Near the Stagnation Point. NASA TR R-8, 1959. (Supersedes NACA TN 4391.)
- 21. Roberts, Leonard: A Theoretical Study of Stagnation-Point Ablation. NASA TR R-9, 1959. (Supersedes NACA TN 4392.)
- \* 22. Swann, Robert T.; and South, Jerry: A Theoretical Analysis of Effects of Ablation on Heat Transfer to an Arbitrary Axisymmetric Body. NASA TN D-741, 1961.
- ✓ 23. Swann, Robert T.: Effect of Thermal Radiation From a Hot Gas Layer on Heat of Ablation. Jour. Aerospace Sci. (Readers' Forum), vol. 28, no. 7, July 1961, pp. 582-583.
- ✓ 24. Savin, Raymond C.; Gloria, Hermilo R.; and Dahms, Richard G.: Ablative Properties of Thermoplastics Under Conditions Simulating Atmosphere Entry of Ballistic Missiles. NASA TM X-397, 1960.
- 25. Dusenberre, G. M.: Numerical Methods for Transient Heat Flow. Trans. A.S.M.E., vol. 67, no. 8, Nov. 1945, pp. 703-712.

3/12/25  
SD

*"The aeronautical and space activities of the United States shall be conducted so as to contribute . . . to the expansion of human knowledge of phenomena in the atmosphere and space. The Administration shall provide for the widest practicable and appropriate dissemination of information concerning its activities and the results thereof."*

—NATIONAL AERONAUTICS AND SPACE ACT OF 1958

## NASA SCIENTIFIC AND TECHNICAL PUBLICATIONS

**TECHNICAL REPORTS:** Scientific and technical information considered important, complete, and a lasting contribution to existing knowledge.

**TECHNICAL NOTES:** Information less broad in scope but nevertheless of importance as a contribution to existing knowledge.

**TECHNICAL MEMORANDUMS:** Information receiving limited distribution because of preliminary data, security classification, or other reasons.

**CONTRACTOR REPORTS:** Technical information generated in connection with a NASA contract or grant and released under NASA auspices.

**TECHNICAL TRANSLATIONS:** Information published in a foreign language considered to merit NASA distribution in English.

**TECHNICAL REPRINTS:** Information derived from NASA activities and initially published in the form of journal articles.

**SPECIAL PUBLICATIONS:** Information derived from or of value to NASA activities but not necessarily reporting the results of individual NASA-programmed scientific efforts. Publications include conference proceedings, monographs, data compilations, handbooks, sourcebooks, and special bibliographies.

*Details on the availability of these publications may be obtained from:*

SCIENTIFIC AND TECHNICAL INFORMATION DIVISION  
NATIONAL AERONAUTICS AND SPACE ADMINISTRATION  
Washington, D.C. 20546